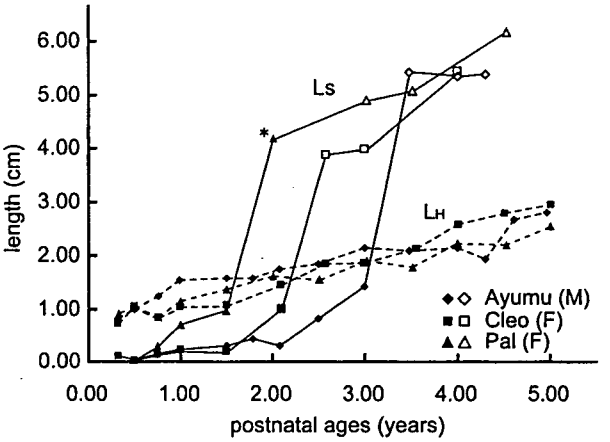

Fig. 3 Growth of the laryngeal sac in 3 chimpanzees: Ayumu (male, diamonds); Cleo (female, triangles), and Pal (female, squares). L_H=length of the hyoidal recess; L_S=length of the suprasternal recess of the sac. We could not measure L_S at some points because the landmarks were out of the image. Open symbols mean that the sac had already expanded beyond the superior edge of the sternum. The sac reached almost the superior edge of the stemoid at 2 yr of in Pal (*; Fig. 2c). In early infancy, the laryngeal sac grows gradually to form the configuration that most adult primate species having a sac show. After late infancy, the sac expands rapidly in the great apes. See also the definitions in Methods.

Discussion

MRI showed 2 distinct phases in the growth of the laryngeal air sac in chimpanzees. In early infancy, the laryngeal sac grows gradually to expand superiorly to the dorsal area of the body of the hyoid and then to extend inferiorly along the ventral aspect of the laryngeal cartilages. Many nonhominoid primates show such a configuration, despite differences in the forms of the sac. Despite controversies regarding the distributions of each type, depending on species, they have a subhyoid sac extending from a ventral midsagittal opening just above the glottis, an infraglottal sac forming from a ventral midsagittal opening between the thyroid and cricoid cartilages, a dorsal sac from a dorsal infraglottal opening between the cricoid cartilage and the first tracheal ring, or they may show bilateral supraventricular sacs arising from bilateral fissures above the ventricles (Hayama 1970; Hewitt *et al.* 2002; Negus 1949; Starck and Schneider 1960). The sac expands within the laryngeal in most species, and at its largest, it expands within the neck (Geist 1965; Hayama 1970; Hewitt *et al.* 2002; Hill and Booth 1957; Negus 1949; Starck and Schneider 1960; Tucker and Tucker 1975). By contrast, from late infancy, the chimpanzees showed a rapid expansion of the sac along the trachea and beyond the neck, despite the slight differences in the timing between subjects. Though we did not evaluate it, the growth phase possibly continues quite early in development to form a sac expanding into the pectoral, clavicular, and axillary regions. Siamang (*Synphalangus syndactylus*) have a ventricular sac, as in great apes, and their sac expands in part to reach the sternum (Hayama 1970; Marler and Tenaza 1977). A ventricular sac may therefore have an advantage over the other forms in enlargement of the laryngeal sac. However, siamang probably do not share the rapid growth phase, so their sac shows no large expansion. Thus, the rapid growth phase in late infancy is

likely a derived phase that contributes principally to the formation of the enlarged sac in chimpanzees.

We found that the rapid growth phase of the laryngeal sac started in the 2 female subjects earlier than in the male, but it remains unclear whether this depends on the sexual dimorphism of the sac. In all great apes and siamang, both males and females have a similar configuration of the sac (Hayama 1970). However, all great apes probably show sexual dimorphism in the volume of the sac, which in turn depends on sexual dimorphism in body size. They also show sex-related differences in behavior patterns involving the laryngeal sac; e.g., inflation of the sac for resonance of thoracic percussion during drumming in male gorillas, and for size exaggeration displays in male orangutans (Marler and Tenaza, 1977; Tuttle 1986). Such differences might depend on sexual dimorphism in volume, but there is little information on the issue. Future studies using large longitudinal samples are necessary to determine whether sexual differences in developmental patterns might contribute to adult sexual dimorphism in sac volumes.

The sacs reached the dorsal region of the hyoidal body by 4 mo in all subjects, but we could not evaluate the time of fusion of the bilateral growing sacs. Avril (1963), using 6 chimpanzee cadavers ranging from the fetal to the subadult stage (Table I), found that the unilateral sac expands greatly and that another sac extends ventrally to fuse with it in the late juvenile period, suggesting that a unilateral sac would have expanded rapidly in late infancy in the subjects examined here. If this is true, fusion of the bilateral sacs by itself can have no influence on the rapid expansion of a sac in chimpanzees. However, the fusion in juvenile or adult periods may modify the functions of a unilateral large sac that has already expanded.

There is little information on the growth patterns of the large sac for other great apes (Table I). Adult gorillas have a configuration of the sac that is almost the same as that in chimpanzees (Avril 1963; Kleinschmidt 1938; Raven 1950). By contrast, orangutans have a different configuration, in which bilateral sacs extend inferiorly from the ventricles to the neck region and fuse in the pectoral region (Avril 1963; Brandes 1932; Huber 1931). However, in orangutans the unilateral sac expands greatly, and another sac expands inferiorly to fuse with it in the late juvenile period, as with chimpanzees (Brandes 1932; Huber 1931). Thus, though there are slight differences in the sac configuration, all the great apes possibly share a rapid expansion of the unilateral sac in late infancy.

The functions of the laryngeal sac in primates are still a matter of debate. Suggested functions include storage of expired air to increase oxygen uptake (Negus 1949) or reduction of the hyperventilation caused by a long sequence of repetitive loud calls (Hewitt *et al.* 2002), generating another sound source in the laryngeal ventricles (Brandes 1932; Huber 1931; Fitch and Hauser 2003; Kelemen 1948), resonating the laryngeal voice source to help produce loud and long calls (Gautier 1971; Fitch and Hauser 2003; Marler and Tenaza 1977; Napier and Napier 1985; Schön 1971; Schön Ybarra 1995), or buffering against the pressure induced by intensive expiratory airflow following air trapping during 3-dimensional arboreal locomotion (Hayama 1970; 1996). These functions excluding the first and last are relevant to vocalization. Though current analysis techniques and acoustic theory need to address such hypotheses (Lieberman 2006; Riede *et al.* 2006), vocal behavior patterns in great apes have attracted particular attention to the major

functions of the enlarged sac in adults (Brandes 1932; Fitch and Hauser 2003; Hewitt *et al.* 2002; Huber 1931; Kelemen 1948; Marler and Tenaza 1977). However, an enlarged sac may not necessarily have evolved to be advantageous for an aspect of vocalization. Though the mature sac probably serves some of the aforementioned functions in adults, separate functions could have arisen-or disappeared-with each developmental event of the sac; e.g., gradual growth in early infancy, rapid expansion in late infancy, or fusion of the bilateral sacs in the late juvenile period. Thus, we suggest that, among the phases, physiological changes accompanying the rapid expansion of the sac in late infancy are likely to shed light on the original functional adaptations of the enlarged sac in the common ancestor of the extant great apes.

Despite differences in effect, the functions principally depend on some physiological modifications in the laryngeal region, including activities of related musculature and manipulation of the airflow. Unfortunately, few studies have evaluated growth-related changes in physiology in the laryngeal region in chimpanzees, probably because of technical limitations. Such studies on infants, not on juveniles and adults, promise to provide valuable insight into the original functional adaptations of the enlarged sac in the great apes and its apparent evolutionary loss in humans.

Acknowledgments We thank A. Kato, K. Kumazaki, N. Maeda, S. Goto, C. Hashimoto, and K. Matsubayashi, M. Tomonaga, M. Tanaka, Y. Hamada, and other staff of Primate Research Institute, Kyoto University (PRI) for permission for or help with the MRI examinations of 3 chimpanzee infants. We performed portions of this work at PRI under PRI Cooperative Research Programs (grant 4–1, 3–1 to T. Nishimura). A Research Fellowship of the Japan Society for the Promotion of Science (JSPS) for Young Scientist (grant 16000326 to T. N.), JSPS Core-to-Core program HOPE (grant 15001 to PRI), and Grants-in-Aid for Specially Promoted Research (grants 1200200916002001 to T. M.) and for the Biodiversity Research of the 21st Century Center of Excellence (grant A14 to Kyoto University) from the Ministry of Education, Culture, Sports, Sciences, and Technology of Japan provided financial support for the work.

References

Avril, C. (1963). Kehlkopf und Kehlsack des Schimpansen, *Pan troglodytes* (Blumenbach 1799). *Gegenbaurs Morphologisches Jahrbuch, 105*, 74–129.

Brandes, R. (1932). Über den Kehlkopf des Orang-Utan in verschiedenen Altersstadien mit besonderer Berücksichtigung der Kehlsackfrage. *Gegenbaurs Morphologisches Jahrbuch, 69*, 1–61.

Fitch, W. T. (2000). The evolution of speech: A comparative review. *Trends in Cognitive Sciences, 4*, 258–267.

Fitch, W. T., & Hauser, M. D. (2003). Unpacking "honesty": Vertebrate vocal production and the evolution of acoustic signals. In A. M. Simmons, A. N. Popper, & R. R., Fay (Eds.), *Acoustic communication* (pp. 65–137). New York: Springer-Verlag.

Gautier, J. P. (1971). Etude morphologique et fonctionnelle des annexes extra-laryngées des Cercopithecinae; liaison avec les cris d'espacement. *Biologia Gabonica, 7*, 229–267.

Geist, F. D. (1965). Nasal cavity, larynx, mouth, and pharynx. In C. G. Hartman, & W. L. Straus Jr., (eds.), *The anatomy of the rhesus monkey* (pp. 189–209) New York: Hafner Publishing.

Gould, S. J. (1977). *Ontogeny and phylogeny.* Belknap Harvard, Cambridge, MA.

Hayama, S. (1970). The *Saccus laryngis* in primates. *Journal of the Anthropological Society of Nippon, 78*, 274–298, (in Japanese with English abstract).

Hayama, S. (1996). Why does not the monkey fall from a tree? The functional origin of the human glottis. *Primate Research, 12*, 179–206. (in Japanese with English abstract)

Hewitt, G., MacLarnon, A., & Jones, K. E. (2002). The functions of laryngeal air sac in primates: A new hypothesis. *Folia Primatologica, 73*, 70–94.

Hill, W. C. O., & Booth, A. H. (1957). Voice and larynx in African and Asiatic colobidae. *Journal of the Bombay Natural History Society, 54*, 309–321.

Huber, E. (1931). *Evolution of Facial Musculature and Expression.* The Johns Hopkins University Press, Baltimore.

Kelemen, G. (1948). The anatomical basis of phonation in the chimpanzee. *Journal of Morphology, 82*, 229–256.

Kleinschmidt, A. (1938). Die Schlund-und Kehlorgane des Gorillas "Bobby" unter besonderer Berücksichtigung der gleichen Organe von Mensch und Orang. *Gegenbaurs Morphologisches Jahrbuch, 81*, 78–157.

Lieberman, P. (2006). Limits on tongue deformation-Diana money formants and the impossible vocal tract shapes proposed by Riede *et al.* (2005). *J. Human Evolution, 50*, 219–221.

Marler, P., & Tenaza, R. (1977). Signaling behavior of apes with special reference to vocalization. In T. A. Sebeok (ed.), *How animals communicate* (pp. 965–1033) Indiana University Press, Bloomington.

Matsuzawa, T. (2003). The Ai project: Historical and ecological contexts. *Animal cognition, 6*, 199–211.

McKinney, M. L., & McNamara, K. J. (1991). *Heterochrony: The evolution of ontogeny.* Plenum Press, New York.

Napier, J. R., & Napier, P. H. (1985). *The natural history of the primates.* Cambridge, MA: MIT Press.

Negus, V. E. (1949). *The Comparative Anatomy and Physiology of the Larynx.* London: William Heinemann Medical Books.

Némai, J., & Kelemen, G. (1933). Beiträge zur Kenntnis des Gibbonkehlkopfes. *Zeitschrift fuÉr Anatomie und Entwicklungsgeschichte, 100*, 512–520.

Nishimura, T., Mikami, A., Suzuki, J., & Matsuzawa, T. (2003). Descent of the larynx in chimpanzee infants. *Proceedings of the National Academy of Sciences, USA, 100*, 6930–6933.

Nishimura, T., Mikami, A., Suzuki, J., & Matsuzawa, T. (2006). Descent of the hyoid in chimpanzees: evolution of face flattening and speech. *Journal of Human Evolution, 51*, 244–254.

Primate Research Institute, Kyoto University. (1986). *Guide for the care and use of laboratory primates.* Primate Research Institute, Kyoto University, Inuyama, Japan.

Primate Research Institute, Kyoto University. (2002). *Guide for the care and use of laboratory primates,* 2nd ed. Primate Research Institute, Kyoto University, Inuyama, Japan.

Raven, H. C. (1950). *The Anatomy of the Gorilla.* Columbia University Press, New York.

Rice, S. H. (2000). The analysis of ontogenetic trajectories: When a change in size or shape in not heterochrony. *Proceedings of the National Academy of Sciences of the United States of America, 94*, 907–912.

Riede, T., Bronson, E. Hatzikirou, H., & Zuberbühler, K. (2006). Multiple discontinuities in nonhuman vocal tracts—A response to Lieberman (2006). *Journal of Human Evolution, 50*, 222–225.

Schön, M. A. (1971). The anatomy of the resonating mechanism in howling monkeys. *Folia Primatologica, 15*, 117–132.

Schön Ybarra, M. A. (1995). A comparative approach to the non-human primate vocal tract: Implications for sound production. In E. Zimmerman, J. D. Newman, & U. Jürgens (eds.), *Current Topics in Primate Vocal Communication.* Plenum Press, New York, pp. 185–198.

Starck, D., & Schneider, R. (1960). Respirationsorgane: A. Larynx. In H., Hofer, A. H., Schultz, & D. Starck (eds.), *Primatologia, Vol. 3–2.* Karger, Basel, pp. 423–587.

Tucker, G., & Tucker, J. A. (1975). Observations on the primate hyoepiglottic complex. *Annals of Otology, Rhinology & Laryngology, 84*, 827–832.

Tuttle, R. H. (1986). *Apes of the world: Their social behavior, communication, mentality, and ecology.* Noyes Publications, Park Ridge, NJ.

Available online at www.sciencedirect.com
ScienceDirect
Behavioural Brain Research 179 (2007) 167–171
BEHAVIOURAL BRAIN RESEARCH
www.elsevier.com/locate/bbr

Research report

Involvement of glial cell line-derived neurotrophic factor in inhibitory effects of a hydrophobic dipeptide Leu-Ile on morphine-induced sensitization and rewarding effects

Minae Niwa[a], Atsumi Nitta[a], Liya Shen[b], Yukihiro Noda[a,c], Toshitaka Nabeshima[a,*]

[a] *Department of Neuropsychopharmacology and Hospital Pharmacy, Nagoya University Graduate School of Medicine, 65 Tsuruma-cho, Showa-ku, Nagoya 466-8560, Japan*
[b] *Laboratory of Cellular Carcinogenesis and Tumor Promotion, Center for Cancer Research, NCI, Bethesda, MD 20983, USA*
[c] *Division of Clinical Science in Clinical Pharmacy Practice, Management and Research, Faculty of Pharmacy, Meijo University, Nagoya 468-8503, Japan*

Received 13 December 2006; received in revised form 24 January 2007; accepted 30 January 2007
Available online 3 February 2007

Abstract

There are few efficacious medications for drug dependence at present. We have previously demonstrated that Leu-Ile, which induces the expression of not only tumor necrosis factor-α (TNF-α) but also glial cell line-derived neurotrophic factor (GDNF), inhibits methamphetamine (METH) and morphine (MOR)-induced sensitization and rewarding effects by regulating extracellular dopamine levels *via* the induction of TNF-α expression, and indicated the potential of Leu-Ile as a novel therapeutic agent for METH and MOR-induced dependence. In the present study, we investigated the involvement of GDNF in inhibitory effects of Leu-Ile on MOR-induced sensitization and rewarding effects. Repeated treatment with MOR for 9 days, which results in an enhancement of the locomotor-stimulating effects (sensitization) of MOR, increased GDNF levels in the nucleus accumbens compared with those in saline-treated mice. Repeated pre-treatment with Leu-Ile for 9 days potentiated the MOR-induced increase in GDNF levels. MOR at a low dose (3 mg/kg) produced place preference in GDNF heterozygous knockout (GDNF-(+/−)) mice, but not in littermate GDNF-(+/+) mice. No inhibitory effect of Leu-Ile on MOR-induced place preference was observed in GDNF-(+/−) mice. These results suggest that GDNF is involved in the inhibitory effects of Leu-Ile on MOR-induced sensitization and rewarding effects.

Keywords: Morphine (MOR); Glial cell line-derived neurotrophic factor (GDNF); Sensitization; Rewarding effects; Leu-Ile; Mice

1. Introduction

Drugs of abuse are able to elicit compulsive drug-seeking behaviors upon repeated administration, which ultimately leads to the phenomenon of addiction. Evidence indicates that the susceptibility to develop addiction is influenced by sources of reinforcement, variable neuroadaptive mechanisms, and neurochemical changes that together lead to altered homeostasis of the brain reward system [7].

Neurotrophic factors and cytokines, which are known to influence synaptic transmission and neuronal morphology [1,2,12], may be involved in alterations of the morphology of dendrites and dendritic spines in the nucleus accumbens (NAc) and prefrontal cortex after repeated injections of psychostimulants [18,19]. Glial cell line-derived neurotrophic factor (GDNF) inhibits the cocaine-induced upregulation of tyrosine hydroxylase (TH) activity in the ventral tegmental area (VTA) and blocks behavioral responses to cocaine [10]. GDNF would be a candidate for therapeutic agents against drug dependence. However, there are serious obstacles to its therapeutic application: it is difficult to deliver GDNF from the periphery to the brain, since it is a macromolecule that cannot penetrate the blood–brain barrier

Abbreviations: CPP, conditioned place preference; DA, dopamine; EIA, enzyme immunoassay; GDNF, glial cell line-derived neurotrophic factor; METH, methamphetamine; MOR, morphine; NAc, nucleus accumbens; TNF-α, tumor necrosis factor-α; TH, tyrosine hydroxylase; VTA, ventral tegmental area

* Corresponding author. Tel.: +81 52 744 2674; fax: +81 52 744 2979.
E-mail address: tnabeshi@med.nagoya-u.ac.jp (T. Nabeshima).

0166-4328/$ – see front matter © 2007 Elsevier B.V. All rights reserved.
doi:10.1016/j.bbr.2007.01.026

[8], and is easily broken down by proteases in the blood stream. Therefore, GDNF cannot be used directly as a therapeutic tool for drug dependence. We hypothesized that a low-molecular-weight compound which induces production of GDNF in the brain could be a novel therapeutic agent for drug dependence.

Recently, we have demonstrated that Leu-Ile, which induces the expression of tumor necrosis factor-α (TNF-α) and GDNF, inhibits methamphetamine (METH)-induced sensitization and rewarding effects by negating the METH-induced inhibition of dopamine (DA) uptake as well as attenuating the METH-induced increase in extracellular DA levels in the NAc *via* the induction of TNF-α and GDNF expression [15]. Moreover, we have demonstrated that Leu-Ile inhibits MOR-induced sensitization and rewarding effects by regulating extracellular DA levels *via* the induction of TNF-α expression [14].

In the present study, to extend our findings, we examined the involvement of GDNF in addition to TNF-α in inhibitory effects of Leu-Ile on MOR-induced sensitization and rewarding effects.

2. Materials and methods

2.1. Reagents

GDNF as a standard for the enzyme immunoassay (EIA) was donated by Amgen (CA, USA). Leu-Ile was purchased from Kokusan Chemical Co., Ltd. (Tokyo, Japan). All other materials used were of reagent grade.

2.2. Animals

Animals were housed in plastic cages and kept in a temperature-, humidity-, and light-controlled room (23 ± 1 °C; 50 ± 5% humidity; 12:12 h light/dark cycle starting at 8:00 a.m.) and had free access to food and water, except during behavioral experiments. All animals' care and use were in accordance with the National Institutes of Health Guide for the Care and Use of Laboratory Animals and were approved by the Institutional Animal Care and Use Committee of Nagoya University School of Medicine. Animals were treated according to the Guidelines of Experimental Animal Care issued from the Office of the Prime Minister of Japan.

The wild-type C57BL/6J mice were obtained from Slc Japan (Hamamatsu, Japan).

Male C57BL/6J-GDNF heterozygous knockout (GDNF-(+/−)) mice, 8–12 weeks of age, were used in the experiments. GDNF-(+/−) were generated as described previously [17]. GDNF (−/−) homozygous knockout mice die shortly after birth (postnatal 7 days), but GDNF (+/−) mice are viable. GDNF levels in the frontal cortex, NAc, caudate putamen, and hippocampus of GDNF-(+/−) mice are 54.8, 65.4, 59.0, and 66.8%, respectively, of those in littermate GDNF-(+/+) mice [15]. Littermate GDNF-(+/+) mice were used as controls in the behavioral experiments.

2.3. Locomotor activity

Locomotor activity was measured using an infrared detector (Neuroscience Co., Ltd., Tokyo, Japan) in a plastic box (32 cm × 22 cm × 15 cm high) [11,14]. Mice were administered Leu-Ile (1.5 and 15 μmol/kg, i.p.) or vehicle, and habituated for 1 h in the box. Mice were administered MOR (10 mg/kg, s.c.) or saline 1 h after the Leu-Ile administration, and the locomotor activity was measured for 2 h immediately after the MOR or saline administration [14]. Leu-Ile and MOR were injected once a day for 9 days.

2.4. Enzyme immunoassay

GDNF levels were measured using an EIA with a minor modification [13]. Mice were administered Leu-Ile (1.5 and 15 μmol/kg, i.p.) once a day 1 h before MOR (10 mg/kg, s.c.) treatment for 9 days and decapitated 24 h after the last administration of MOR (Fig. 1A). Homogenate buffer (0.1 M Tris–HCl [pH 7.4] containing 1 M NaCl, 2% bovine serum albumin, 2 mM EDTA, and 0.2% Na_3N) was added to brain tissue at a ratio of 1 g wet weight per 19 ml of buffer, pulse-sonicated for 100 s, and centrifuged at 100,000 × *g* for 30 min. The supernatant was collected and used for the EIA.

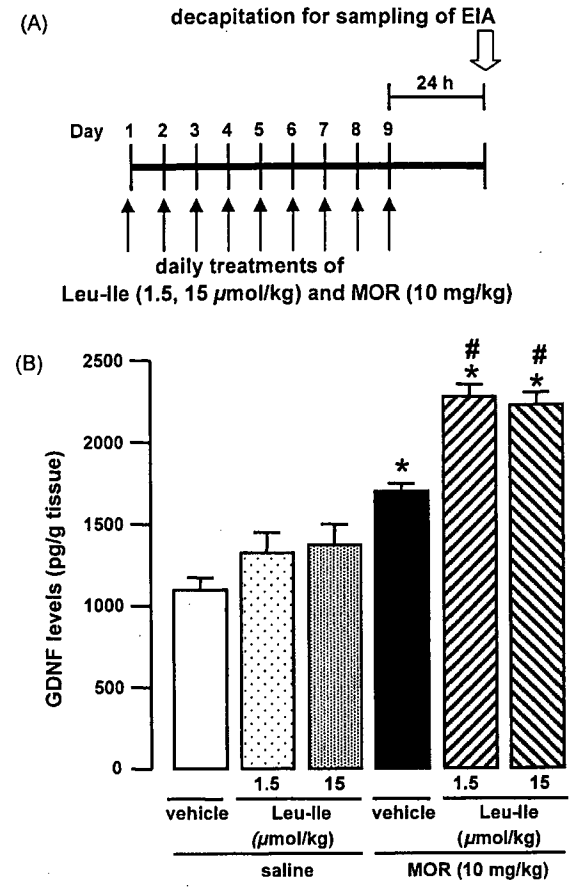

Fig. 1. Effect of Leu-Ile on morphine (MOR)-induced increase in glial cell line-derived neurotrophic factor (GDNF) levels. (A) Experimental schedule for measurement of GDNF levels using the enzyme immunoassay (EIA) method. Mice were treated with Leu-Ile (1.5 and 15 μmol/kg, i.p.) or vehicle 1 h before MOR (10 mg/kg, s.c.) or saline once a day for 9 days and decapitated 24 h after the last MOR or saline administration. (B) Change of GDNF levels in the nucleus accumbens after the administration of Leu-Ile and/or MOR. Values are mean ± S.E. ($n = 6$–8). $^{*}p < 0.05$ vs. vehicle/saline-treated mice. $^{\#}p < 0.05$ vs. vehicle/MOR-treated mice.

2.5. Conditioned place preference

The apparatus used for the place conditioning task consisted of two compartments: a transparent Plexiglas box and a black Plexiglas box (both 15 cm × 15 cm × 15 cm high). To enable mice to distinguish easily the two compartments, the floors of the transparent and black boxes were covered with white plastic mesh and black frosting Plexiglas, respectively. Each box could be divided by a sliding door (10 cm × 15 cm high). The place conditioning paradigm was performed by using a previously established procedure [14,16]. The experimental schedule for the conditioned place preference (CPP) task is shown in Fig. 2A. In the pre-conditioning test, the sliding door was opened, and the mouse was allowed to move freely between both boxes for 15 min once a day for 3 days. On the third day of the pre-conditioning test, we measured the time that the mouse spent in the black and transparent boxes by using a Scanet SV-20 LD (Melquest Co., Ltd., Toyama, Japan). The box in which the mouse spent the most time was referred to as the "preferred side", and the other box as the "non-preferred side". Conditioning was performed during six successive days.

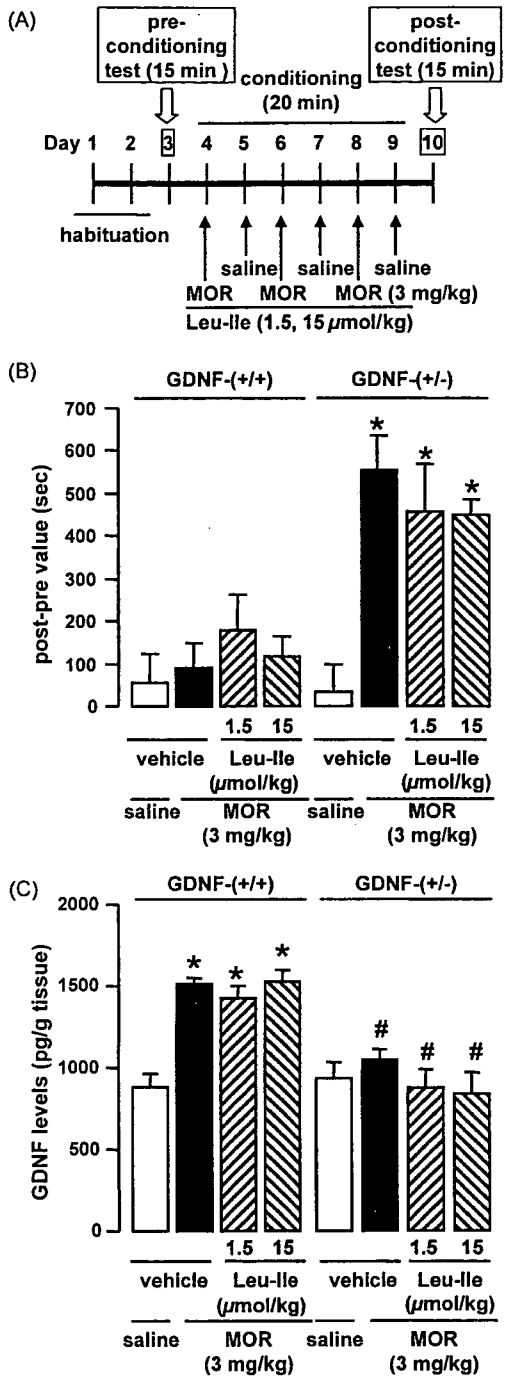

Fig. 2. Effect of Leu-Ile on MOR-induced place preference in GDNF-(+/−) mice. (A) Experimental schedule for the conditioned place preference task. On the third day of the pre-conditioning test, we measured the time that the mouse spent in the black and transparent boxes. Mice were subcutaneously given MOR (3 mg/kg, s.c.) and put in its non-preferred side for 20 min. On the next day, the mouse was given saline and placed opposite the drug conditioning site for 20 min. These treatments were repeated for three cycles (6 days). In the post-conditioning test, the sliding door was opened, and we measured the time that the mouse spent in the black and transparent boxes for 15 min. Closed arrows indicate the days of MOR or saline administration. Mice were treated with Leu-Ile (1.5 and 15 μmol/kg, i.p.) or vehicle 1 h before MOR (3 mg/kg, s.c.) or saline administration. (B) Effect of Leu-Ile treatment on MOR-induced place preference in GDNF-(+/−) mice. Mice were co-treated with Leu-Ile and MOR in the conditioning phase. Mice were treated with Leu-Ile (1.5 and 15 μmol/kg, i.p.) 1 h before MOR (3 mg/kg, s.c.) or saline administration. Values are means ± S.E. (n = 10–14). $^{*}p < 0.05$ vs. vehicle/MOR-treated GDNF-(+/+) mice. (C) Change of GDNF levels in the NAc after post-conditioning test in conditioned place preference paradigm. Mice were co-treated with Leu-Ile (1.5 and 15 μmol/kg, i.p.) and MOR (3 mg/kg, s.c.) in the conditioning period and decapitated 24 h after post-conditioning test. Values are means ± S.E. (n = 5). $^{*}p < 0.05$ vs. vehicle/saline-treated GDNF-(+/+) mice. $^{\#}p < 0.05$ vs. vehicle/MOR-treated GDNF-(+/+) mice. Abbreviations as in Fig. 1.

Mice were given MOR or saline in the apparatus with the sliding door closed. That is, a mouse was subcutaneously given MOR and put in its non-preferred side for 20 min. On the next day, the mouse was given saline and placed opposite the drug conditioning site for 20 min. These treatments were repeated for three cycles (6 days). In the post-conditioning test, the sliding door was opened, and we measured the time that the mouse spent in the black and transparent boxes for 15 min, using the Scanet SV-20 LD. Place conditioning behavior was expressed by post–pre, which was calculated as: [(post-value) − (pre-value)], where post- and pre-values were the difference in time spent at the drug conditioning and the saline conditioning sites in the post-conditioning and pre-conditioning tests, respectively.

2.6. Statistical analysis

All data were expressed as means ± S.E. Statistical differences among more than three groups were determined using a one-way analysis of variance (ANOVA), followed by the Bonferroni multiple comparison test. $p < 0.05$ was regarded as statistically significant.

3. Results

3.1. Effect of Leu-Ile on MOR-induced increase in GDNF levels

Single MOR treatment at the dose of 10 mg/kg increases locomotor activity, and repeated administration for 9 days results in an enhancement of the locomotor-stimulating effect of MOR (sensitization) [14]. Leu-Ile (1.5 and 15 μmol/kg, i.p.) inhibits the MOR-induced hyperlocomotion and sensitization [14]. The sensitization to the locomotor-stimulating effects is argued to reflect one neuroadaptive process associated with dependence. To confirm the involvement of GDNF in the inhibitory effects of Leu-Ile on MOR-induced sensitization, GDNF levels in the NAc were determined after the co-administration of Leu-Ile and MOR using the EIA method. MOR (10 mg/kg) increased GDNF levels in the NAc compared with those in the vehicle/saline-treated mice. GDNF levels after the co-administration of Leu-Ile (1.5 and 15 μmol/kg, i.p.) and MOR (10 mg/kg) were much more increased compared with those in the vehicle/MOR-treated mice ($F_{(5,38)} = 28.1$, $p < 0.05$, one-way ANOVA) (Fig. 1B). These results suggest that GDNF is involved in the effects of Leu-Ile on the sensitization.

3.2. Effect of Leu-Ile on MOR-induced place preference in GDNF-(+/−) mice

We have investigated the effects of Leu-Ile on the rewarding effects of MOR in the CPP paradigm, in which animals learn the association of an environment paired with drug exposure. Therefore, CPP is considered a measure of the rewarding properties of drugs of abuse. Leu-Ile (1.5 μmol/kg, i.p.) inhibits

MOR-induced place preference in C57BL/6J mice [14]. The involvement of GDNF in the rewarding effects of MOR and the inhibitory effects of Leu-Ile on MOR-induced place preference were examined in GDNF-(+/−) mice. The experimental schedule is described in Fig. 2A. As shown in Fig. 2B, at the low dose of MOR (3 mg/kg, s.c.), GDNF-(+/−) mice developed place preference, although littermate control GDNF-(+/+) mice did not ($F_{(7,86)} = 7.6$, $p < 0.05$, one-way ANOVA). When Leu-Ile (1.5 and 15 μmol/kg, i.p.) was administered 1 h before MOR, it failed to exhibit a significant effect on the action of MOR in GDNF-(+/−) mice (Fig. 2B). We measured the GDNF levels in the NAc after CPP test using EIA methods. As shown in Fig. 2C, in the NAc of GDNF-(+/+) mice, administration of MOR (3 mg/kg, s.c.) during conditioning phase in CPP test increased GDNF levels compared with vehicle/saline-treated mice ($F_{(7,32)} = 12.1$, $p < 0.05$, one-way ANOVA). Moreover, Leu-Ile increased GDNF levels in combination with MOR (3 mg/kg, s.c.) in CPP paradigm compared with vehicle/saline-treated GDNF-(+/+) mice (Fig. 2C). Conversely, in the NAc of GDNF-(+/−) mice, we confirmed that administration of MOR (3 mg/kg, s.c.) during conditioning phase in CPP test, which could develop place preference, failed to increase GDNF levels. Moreover, Leu-Ile, which could not inhibit rewarding effects of MOR, also failed to increase GDNF levels in combination with MOR in CPP paradigm (Fig. 2C). These results suggest that GDNF acts to negate the rewarding effects of MOR and is involved in the effects of Leu-Ile on the rewarding effects.

4. Discussion

GDNF enhances the survival and maintains the differentiated properties of dopaminergic neurons in cell cultures. The use of GDNF appears to be a promising strategy to promote the survival and function of the nigrostriatal dopaminergic pathway damaged in Parkinson's disease [6]. Transplantation of simian virus-40 glial cells, which produces and secretes GDNF, or delivery of GDNF-conjugated nanoparticles into dorsal and ventral striatum impairs the acquisition of cocaine self-administration in rats [3,4]. The upregulation of the GDNF pathway in the midbrain, is the molecular mechanism by which the putative anti-addiction drug ibogaine mediates its desirable action of reducing ethanol consumption [5]. Infusion of GDNF into the VTA blocks certain biochemical adaptations (induction of TH, NR1 subunit of *N*-methyl D-aspartate receptors, ΔFosB and protein kinase A catalytic subunit) to chronic cocaine or MOR treatment as well as cocaine-induced place preference [10]. Conversely, responses to cocaine are enhanced in rats by intra-VTA infusion of anti-GDNF antibody and in GDNF-(+/−) mice [10]. GDNF has pronounced effects on the dopaminergic system *in vivo*, including neuroprotective effects against METH-induced neurotoxicity [20]. However, as said at the beginning of this article, GDNF cannot be used directly as a therapeutic tool for drug dependence.

Recently, we have demonstrated that Leu-Ile, which induces the expression of TNF-α and GDNF, inhibits METH and MOR-induced sensitization and rewarding effects [14,15]. In the present study, to extend our findings, we examined the involvement of GDNF in the inhibitory effects of Leu-Ile on MOR-induced sensitization and rewarding effects.

GDNF levels in the striatum are increased by the intracerebroventricular administration of Leu-Ile in rats [13]. Expression levels of GDNF mRNA are significantly elevated 24 h after Leu-Ile treatment in cultured neurons compared with the control group and GDNF levels after the co-administration of Leu-Ile and METH are significantly increased compared with those in the vehicle/METH-treated mice [15]. Leu-Ile inhibits the MOR-induced locomotor sensitization, at least in part, through the action in the NAc, since it has inhibitory effects on the repeated MOR treatment-induced increase in extracellular DA levels [14]. In the present study, GDNF levels in the NAc were determined after the co-administration of Leu-Ile and MOR using the EIA method. Leu-Ile potentiated MOR-induced increase in GDNF levels (Fig. 1) in addition to TNF-α [14] in the NAc. GDNF inhibits the drug-induced upregulation of tyrosine hydroxylase activity [10]. TNF-α activates plasmalemmal and vesicular DA transporter [11]. Thereby, we suggest that GDNF and TNF-α induced by Leu-Ile attenuate the MOR-induced increase in extracellular DA levels in the NAc and then inhibit MOR-induced sensitization. In addition, Leu-Ile treatment in combination with METH or MOR and after withdrawal from repeated treatment with METH or MOR inhibits place preference and sensitization to METH or MOR [14,15]. GDNF acts to negate the rewarding effects of MOR, since GDNF-(+/−) mice showed greater MOR-induced place preference compared with littermate control mice (Fig. 2A and B). GDNF could be involved in the inhibitory effects of Leu-Ile on the rewarding effects of MOR, since no effects of Leu-Ile were observed in the GDNF-(+/−) mice (Fig. 2A and B) and Leu-Ile failed to increase GDNF levels in combination with MOR in CPP paradigm in the NAc of GDNF-(+/−) mice (Fig. 2C). GDNF blocks the biochemical and behavioral responses to chronic cocaine or MOR exposure [10]. GDNF decreases TH levels in normal animals, suggesting an active down-regulation of the synthesis of this enzyme [9]. These results suggest that Leu-Ile plays an inhibitory role in the rewarding effects and sensitization induced by MOR in addition to METH *via* the induction of GDNF expression.

Our previous findings indicated that Leu-Ile inhibits MOR-induced sensitization and rewarding effects by attenuating the MOR-induced increase in extracellular DA levels *via* the induction of TNF-α expression [14]. In the present study, we demonstrated that GDNF is also involved in the inhibitory effects of Leu-Ile on MOR-induced sensitization and rewarding effects. Taken together, Leu-Ile inhibits MOR-induced sensitization and rewarding effects *via* the induction of not only TNF-α, but also GDNF, expression. Leu-Ile could be a novel therapeutic agent for MOR-induced dependence.

Acknowledgments

This study was supported in part by a Grant-in-aid for Scientific Research and Special Coordination Funds for Promoting Science and Technology, Target-Oriented Brain Science Research Program; by a Grant-in-aid for Scientific Research

(B) and Young Scientists (A); by the 21st Century Center of Excellence Program "Integrated Molecular Medicine for Neuronal and Neoplastic Disorders" from the Ministry of Education, Culture, Sports, Science and Technology of Japan; by a Grant-in-aid for Health Science Research on Regulatory Science of Pharmaceuticals and Medical Devices, and Dementia and Fracture from the Ministry of Health, Labor and Welfare of Japan; by the Japan Society for the Promotion of Science Joint Research Project under the Japan-Korea Basic Scientific Cooperation Program; by a Smoking Research Foundation Grant for Biomedical Research; by the Mochida Memorial Foundation for Medical and Pharmaceutical Research; by a grant from the Brain Research Center from the 21st Century Frontier Research Program funded by the Ministry of Science and Technology, Republic of Korea; and by the Japan Canada Joint Health Research Program.

References

[1] Boulanger L, Poo M. Gating of BDNF-induced synaptic potentiation by cAMP. Science 1999;284:1982–4.
[2] Connor B, Dragunow M. The role of neuronal growth factors in neurodegenerative disorders of the human brain. Brain Res Brain Res Rev 1998;27:1–39.
[3] Green-Sadan T, Kinor N, Roth-Deri I, Geffen-Aricha R, Schindler CJ, Yadid G. Transplantation of glial cell line-derived neurotrophic factor-expressing cells into the striatum and nucleus accumbens attenuates acquisition of cocaine self-administration in rats. Eur J Neurosci 2003;18:2093–8.
[4] Green-Sadan T, Kuttner Y, Lublin-Tennenbaum T, Kinor N, Boguslavsky Y, Margel S, et al. Glial cell line-derived neurotrophic factor-conjugated nanoparticles suppress acquisition of cocaine self-administration in rats. Exp Neurol 2005;194:97–105.
[5] He DY, McGough NN, Ravindranathan A, Jeanblanc J, Logrip ML, Phamluong K, et al. Glial cell line-derived neurotrophic factor mediates the desirable actions of the anti-addiction drug ibogaine against alcohol consumption. J Neurosci 2005;25:619–28.
[6] Kirik D, Georgievska B, Rosenblad C, Bjorklund A. Delayed infusion of GDNF promotes recovery of motor function in the partial lesion model of Parkinson's disease. Eur J Neurosci 2001;13:1589–99.
[7] Laakso A, Mohn AR, Gainetdinov RR, Caron MG. Experimental genetic approaches to addiction. Neuron 2002;36:213–28.
[8] Lin LF, Doherty DH, Lile JD, Bektesh S, Collins F. GDNF: a glial cell line-derived neurotrophic factor for midbrain dopaminergic neurons. Science 1993;260:1130–2.
[9] Lu X, Hagg H. Glial cell line-derived neurotrophic factor prevents death, but not reductions in tyrosine hydroxylase, of injured nigrostriatal neurons in adult rats. J Comp Neurol 1997;388:484–94.
[10] Messer CJ, Eisch AJ, Carlezon Jr WA, Whisler K, Shen L, Wolf DH, et al. Role for GDNF in biochemical and behavioral adaptations to drugs of abuse. Neuron 2000;26:247–57.
[11] Nakajima A, Yamada K, Nagai T, Uchiyama T, Miyamoto Y, Mamiya T, et al. Role of tumor necrosis factor-α in methamphetamine-induced drug dependence and neurotoxicity. J Neurosci 2004;24:2212–25.
[12] Neumann H, Schweigreiter R, Yamashita T, Rosenkranz K, Wekerle H, Barde Y. Tumor necrosis factor inhibits neurite outgrowth and branching of hippocampal neurons by a Rho-dependent mechanism. J Neurosci 2002;22:854–62.
[13] Nitta A, Nishioka H, Fukumitsu H, Furukawa Y, Sugiura H, Shen L, et al. Hydrophobic dipeptide Leu-Ile protects against neuronal death by inducing brain-derived neurotrophic factor and glial cell line-derived neurotrophic factor synthesis. J Neurosci Res 2004;78:250–8.
[14] Niwa M, Nitta A, Yamada Y, Nakajima A, Saito K, Seishima M, et al. Tumor necrosis factor-α and its inducer inhibit morphine-induced rewarding effects and sensitization. Biol Psychiatry, 2007 Jan 8, [Epub ahead of print].
[15] Niwa M, Nitta A, Yamada Y, Nakajima A, Saito K, Seishima M, et al. An inducer for glial cell line-derived neurotrophic factor and tumor necrosis factor-α protects methamphetamine-induced reward and sensitization. Biol Psychiatry, 2006 Oct 12, [Epub ahead of print].
[16] Noda Y, Miyamoto Y, Mamiya T, Kamei H, Furukawa H, Nabeshima T. Involvement of dopaminergic system in phencyclidine-induced place preference in mice pretreated with phencyclidine repeatedly. J Pharmacol Exp Ther 1998;286:44–51.
[17] Pichel JG, Shen L, Sheng HZ, Granholm AC, Drago J, Grinberg A, et al. Defects in enteric innervation and kidney development in mice lacking GDNF. Nature 1996;382:73–6.
[18] Robinson TE, Kolb B. Persistent structural modifications in nucleus accumbens and prefrontal cortex neurons produced by previous experience with amphetamine. J Neurosci 1997;17:8491–7.
[19] Robinson TE, Kolb B. Alterations in the morphology of dendrites and dendritic spines in the nucleus accumbens and prefrontal cortex following repeated treatment with amphetamine or cocaine. Eur J Neurosci 1999;11:1598–604.
[20] Yamada K, Nabeshima T. Pro- and anti-addictive neurotrophic factors and cytokines in psychostimulant addiction: mini review. Ann NY Acad Sci 2004;1025:198–204.

Available online at www.sciencedirect.com
ScienceDirect
Behavioural Brain Research 180 (2007) 139–145
BEHAVIOURAL BRAIN RESEARCH
www.elsevier.com/locate/bbr

Research report

A natural scavenger of peroxynitrites, rosmarinic acid, protects against impairment of memory induced by $A\beta_{25-35}$

Tursun Alkam[a,b,1], Atsumi Nitta[a,1], Hiroyuki Mizoguchi[a], Akio Itoh[a], Toshitaka Nabeshima[a,c,*]

[a] Department of Neuropsychopharmacology & Hospital Pharmacy, Nagoya University Graduate School of Medicine, Nagoya 466-8560, Japan
[b] Department of Basic Medicine, College of Traditional Uighur Medicine, Hotan 84800, China
[c] Japanese Drug Organization of Appropriate Use and Research, Nagoya 468-0069, Japan

Received 2 January 2007; received in revised form 26 February 2007; accepted 2 March 2007
Available online 12 March 2007

Abstract

Peroxynitrite ($ONOO^-$)-mediated damage is regarded to be responsible for the cognitive dysfunction induced by amyloid beta protein (Aβ) in Alzheimer's disease (AD). In the present study, we examined the protective effects of rosmarinic acid (RA), a natural scavenger of $ONOO^-$, on the memory impairment in a mouse model induced by acute i.c.v. injection of $A\beta_{25-35}$. Mice daily received i.p. several doses of RA after the injection of $A\beta_{25-35}$. RA prevented the memory impairments induced by $A\beta_{25-35}$ in the Y maze test and novel object recognition task. RA, at the effective lowest dose (0.25 mg/kg), prevented $A\beta_{25-35}$-induced nitration of proteins, an indirect indicator of $ONOO^-$ damage, in the hippocampus. At this dose, RA also prevented nitration of proteins and impairment of recognition memory induced by $ONOO^-$-i.c.v.-injection. Co-injection of the non-memory-impairing dose of $ONOO^-$ with $A\beta_{25-35}$ blocked the protective effects of RA (0.25 mg/kg). These results demonstrated that the memory protective effects of RA in the neurotoxicity of $A\beta_{25-35}$ is due to its scavenging of $ONOO^-$, and that daily consumption of RA may protect against memory impairments observed in AD.

Keywords: Rosmarinic acid; Amyloid beta (25–35); Peroxynitrite; Protein nitration; Memory impairment

1. Introduction

Complementary and alternative medicines, with the superiority as natural substances, have increasingly been used for health care and treatment for some chronic diseases. A number of herbs, including *Rosmarinus officinalis* L., *Borago officinalis*, *Melissa officinalis*, and *Salvia officinalis*, are used as an effective treatment against dementia in Traditional Uighur Medicine. Among these herbs, ethanol extracts of *M. officinalis* and *S. officinalis* have been reported to be effective in the management of mild to moderate AD in randomized double-blind clinical studies [1,2]. The principal ethanol-soluble constituent, with the therapeutic effects, of these herbs has been found to be rosmarinic acid (RA) [3,16,18] (Fig. 1). RA is regarded as a daily-consumed safe ingredient, due to its extensive use in food industry for flavouring.

The medicinal value of RA has also been well recognized, especially in regard to its antioxidant and anti-inflammatory activities [21,33,37]. RA displays a strong scavenger activity for $ONOO^-$ and other free radicals [8,21,32]. $ONOO^-$ is responsible for a wide spread biological damage in the brains of AD [6,35]. Aβ, the principal component of the senile plaques, is the main cause of increased $ONOO^-$ in the brain of AD [5,41]. In cell culture studies, RA protects against the reactive oxygen species induced by Aβ [12]. Further, RA not only inhibits the formation of beta-amyloid fibrils (fAβ), but also destabilizes preformed fAβ in vitro [27]. These reports suggest that RA have a beneficial role to reduce the neurotoxicity of Aβ in AD. However, no in vivo investigation on the effects of RA on the cognitive impairment in the neurotoxicity of Aβ has been reported. It is necessary to investigate the effects of RA and

* Corresponding author at: Department of Neuropsychopharmacology & Hospital Pharmacy, Nagoya University Graduate School of Medicine, 65 Tsuruma-cho, Showa-ku, Nagoya 466-8560, Japan. Tel.: +81 52 744 2674; fax: +81 52 744 2682.
E-mail address: tnabeshi@med.nagoya-u.ac.jp (T. Nabeshima).
[1] These authors contributed equally to this work.

0166-4328/$ – see front matter © 2007 Elsevier B.V. All rights reserved.
doi:10.1016/j.bbr.2007.03.001

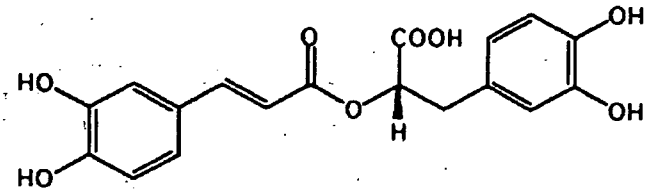

Fig. 1. Chemical structure of rosmarinic acid.

provide experimental basis of its use for Aβ neurotoxicity of AD.

The major component of senile plaques in the brain of AD is $A\beta_{1-40}$ and $A\beta_{1-42}$. The core toxic fragment of full-length $A\beta_{1-40}$ is $A\beta_{25-35}$. $A\beta_{25-35}$ shows faster and stronger, in the similitude with $A\beta_{1-40}$, neurotoxic effects such as oxidative damage, inflammatory responses and memory impairment [7,17,25,30,40,44,47]. In this study, we have therefore evaluated and characterized the antioxidant effects of RA in a mouse model of impaired memory established by the i.c.v.-injection of $A\beta_{25-35}$ [17].

2. Methods

2.1. Animals

Male ICR mice (Nihon SLC Co., Shizuoka, Japan) were used. The animals were housed in a controlled environment (23 ± 1 °C, 50 ± 5% humidity) and allowed food and water ad lib. The room lights were kept on between 8:00 a.m. and 8:00 p.m. All experiments were performed in accordance with the Guidelines for Animal Experiments of Nagoya University Graduate School of Medicine. The procedures involving animals and their care conformed to the international guidelines set out in "Principles of Laboratory Animal Care" (NIH publication no. 85-23, revised 1985).

2.2. Intracerebroventricular injection

$A\beta_{25-35}$ (Bachem, Bubendorf, Switzerland) was dissolved in sterile double-distilled water in a concentration of 1 mg/ml and stored at −20 °C before use. The dissolved $A\beta_{25-35}$ was incubated for aggregation at 37 °C for 4 days. The distilled water was incubated at the same condition as control. Aggregated $A\beta_{25-35}$ (3 μg/3 μl) or incubated distilled water (3 μl) was i.c.v. injected as described previously [17]. Briefly, a microsyringe with a 28-gauge stainless-steel needle 3.0 mm long was used for all experiments. Mice were anesthetized lightly with ether, and the needle inserted unilaterally 1 mm to the right of the midline point equidistant from each eye, at an equal distance between the eyes and the ears and perpendicular to the plane of the skull. A single-shot of the same volume (3 μl) of peptide or vehicle was delivered gradually within 3 s. Mice exhibited normal behavior within 1 min after injection. The administration site was confirmed in preliminary experiments. Neither insertion of the needle nor the volume of injection had a significant influence on survival, and behavioral responses or cognitive functions. $ONOO^-$ (Upstate, Lake placid, NY) was i.c.v. injected at a volume of 1 μl in the same way described above.

2.3. Experimental design

RA (Sigma, USA) was dissolved in physiological saline. Uric acid (UA) (Wako Chemicals, Osaka, Japan) was prepared as suspension in saline. Immediately after the injection of $A\beta_{25-35}$, mice were administrated with RA (0.05, 0.25, 1, 2, and 4 mg/kg day, i.p.) or UA (100 mg/kg, i.p.) daily for 9 consecutive days. Biochemical and behavioral investigations were performed at the indicated time points (see Fig. 2).

2.4. Y-maze test

The Y-maze task was carried out on Day 6 after the injection of $A\beta_{25-35}$, as described previously [45]. Briefly, the apparatus consisted of black-painted plywood. Each arm of the Y-maze was 50 cm long, 12 cm high and 4 cm wide and positioned at an equal angle. Each mouse was placed at the cross-points of arms and allowed to move freely through the maze for an 8-min session. The sequence of arm entries was recorded manually. Spontaneous alternation behavior was defined as the consecutive entry of a mouse into all three different arms (i.e., arm A, arm B, and arm C) to form a triplet of non-repeated components. The percent spontaneous alternation behavior was calculated as the ratio of actual to possible alternations (defined as the total number of arm entries − 2) × 100.

2.5. Novel object recognition task (NORT)

This task, based on the spontaneous tendency of rodents to explore a novel object more often than a familiar one [10], was performed with a slight modification as described previously [9]. A plastic chamber (35 cm × 35 cm × 35 cm) was used in low light condition during the light phase of the light/dark cycle. The general procedure consisted of three different phases: a habituation phase, an acquisition phase, and a retention phase. On the 1st day (habituation phase), mice were individually subjected to a single familiarization session of 10 min, during which they were introduced in the empty arena, in order to become familiar with the apparatus. On the 2nd day (acquisition phase) animals were subjected to a single 10-min session, during which floor-fixed two objects (A and B) were placed in a symmetric position from the centre of the arena, 15 cm from each and 8 cm from the nearest wall. The two objects, made of the same wooden material with the similar color and smell, were different in shape but identical in size. Mice were allowed to explore the objects in the open field. A preference index for each mouse was expressed as a ratio of the amount of time spent exploring object A ($T_A \times 100)/(T_A + T_B$), where T_A and T_B are the time spent on exploring

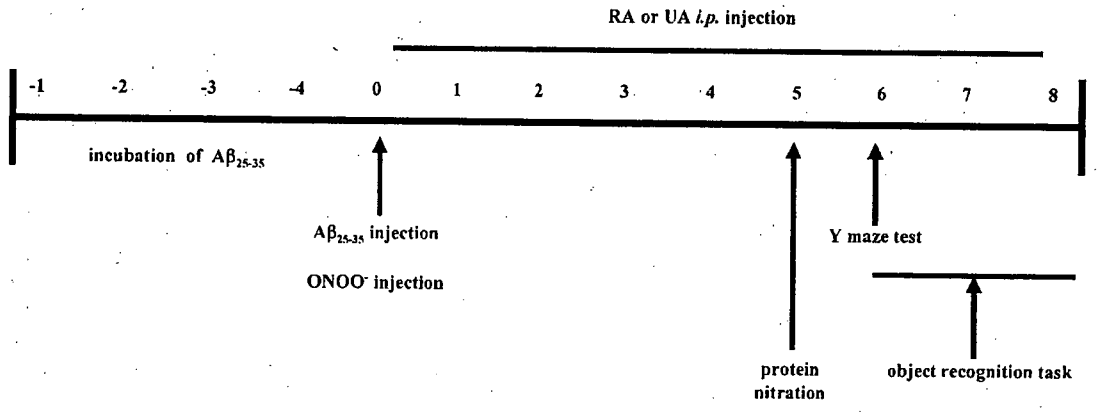

Fig. 2. Experimental schedule.

object A and object B, respectively. On the 3rd day (retention phase), mice were allowed to explore the open field in the presence of two objects: the familiar object A and a novel object C in different shape but in similar color and size (A and C). A recognition index, calculated for each mouse, was expressed as the ratio $(T_C \times 100)/(T_A + T_C)$, where T_A and T_C are the time spent during retention phase on object A and object C, respectively. The time spent exploring the object (nose pointing toward the object at a distance $\leq$1 cm) was recorded by hand.

2.6. Western blotting

Animals were decapitated on Day 5 after the injection of either $A\beta_{25-35}$ or peroxynitrite. The hippocampi were removed on ice-cold glass plate and stored at −80 °C. The hippocampal tissues were homogenized in ice cold extraction buffer (20 mM Tris–HCl buffer (pH 7.6) containing 150 mM NaCl, 2 mM EDTA·2Na, 50 mM sodium fluoride, 1 mM sodium vanadate, 1% NP-40, 1% sodium deoxycholate, 0.1% sodium dodecyl sulphate (SDS), 1 mg/ml pepstatin, 1 mg/ml aprotinin, and 1 mg/ml leupeptin). Twenty microgram of equal amounts protein was resolved by a 7.5% sodium dodecyl sulphate-polyacrylamide gel electrophoresis (SDS-PAGE). The proteins were then transferred electrophoretically to a polyvinylidene difluoride membrane (Millipore Corporation, Billerica, MA). Membranes were incubated in 3% skim milk in phosphate-buffered saline containing 0.05% (v/v) Tween-20 for 2 h at room temperature. Mouse anti-nitrotyrosine antibody, clone 1A6 (Upstate cell signaling, Lake Placid), and goat anti-actin antibodies (Santa Cruz Biotechnology Inc., Santa Crutz, CA) were used to detect nitrated protein and β-actin, respectively. The intensity of each protein band on the film, was analyzed with the Atto Densitograph 4.1 system (Atto, Tokyo, Japan), and was corrected with the corresponding β-actin level. The results were expressed as the percentage of that of the control.

2.7. Statistical analyses

The results are expressed as the mean ± S.E. Statistical significance was determined with one-way ANOVA followed by the Bonferroni multiple comparisons test. $p < 0.05$ was taken as a significant level of difference.

3. Results

3.1. Effects of RA on $A\beta_{25-35}$-induced memory impairment

Based on the reports of pharmacological studies of RA on central nervous system in mice [38,39] and the clinically applying doses of the herbs contained RA, we determined the dose range as 0.05–4 mg/kg day for the selection of optimum dose by behavioral investigation. In the Y-maze test, spontaneous alternation behaviors in $A\beta_{25-35}$ group were significantly less than that in vehicle group while the number of arm entry in each group was the same (Fig. 3A and B). Daily treatment with RA (0.25, 1, 2, and 4 mg/kg) after the injection of $A\beta_{25-35}$ increased the alternation behavior compared to $A\beta_{25-35}$ group (Fig. 3B). In the NORT, all groups explored the two different objects for a similar amount of time during acquisition phase (Fig. 3C). No differences among groups were observed with regards to overall object exploration when different doses of RA were administered (Fig. 3C). During retention phase, the group of

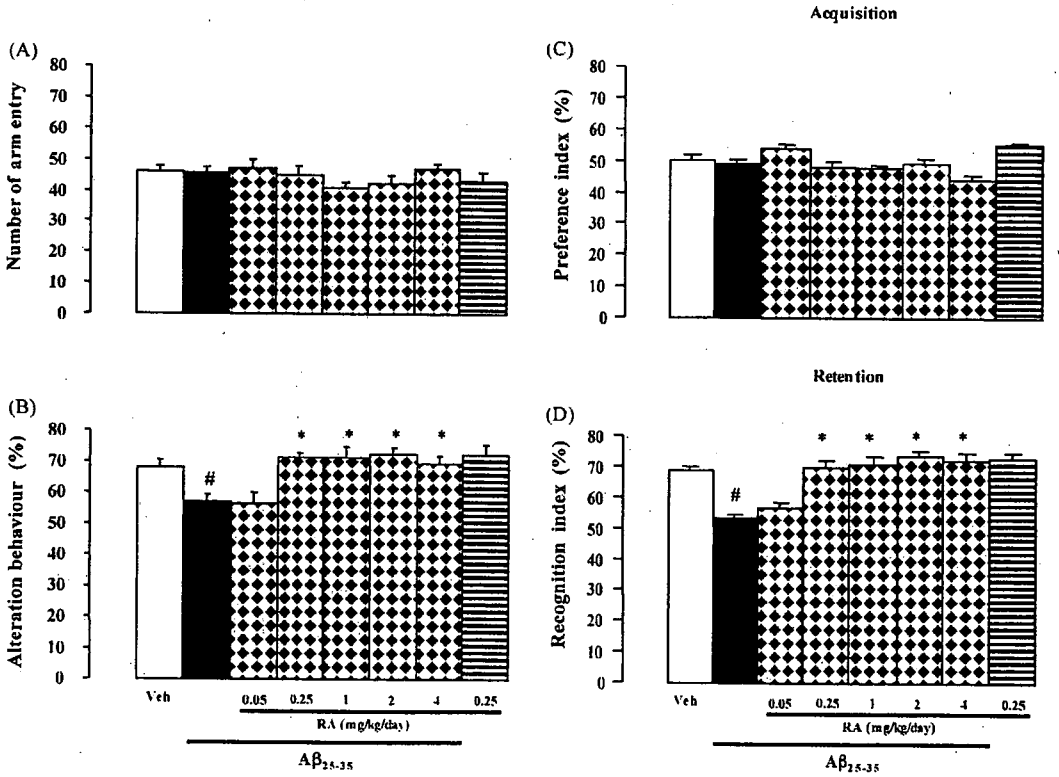

Fig. 3. Effects of rosmarinic acid on the impairment of memory induced by $A\beta_{25-35}$. Various doses of RA were administrated i.p. after i.c.v. injection of $A\beta_{25-35}$ (Day 0) for 9 consecutive days. Mice were subjected to the Y-maze test (A and B) on Day 6 and the NORT (C and D) on Days 6–8. The immediate working memory in the Y-maze test and the long-term memory in the NORT of $A\beta_{25-35}$-injected mice are significantly impaired than those in vehicle i.c.v.-injected mice. Treatment with RA at the doses of 0.25, 1, 2, and 4 mg/kg day significantly prevented the impairment of memory in $A\beta_{25-35}$-injected mice. RA treatment alone did not boost the memory in naive mice. Data were presented as the mean ± S.E. ($n = 10$). $^*p < 0.05$ vs. veh. $^\#p < 0.05$ vs. $A\beta_{25-35}$. Veh: vehicle, RA: rosmarinic acid, $A\beta_{25-35}$: amyloid beta (25–35).

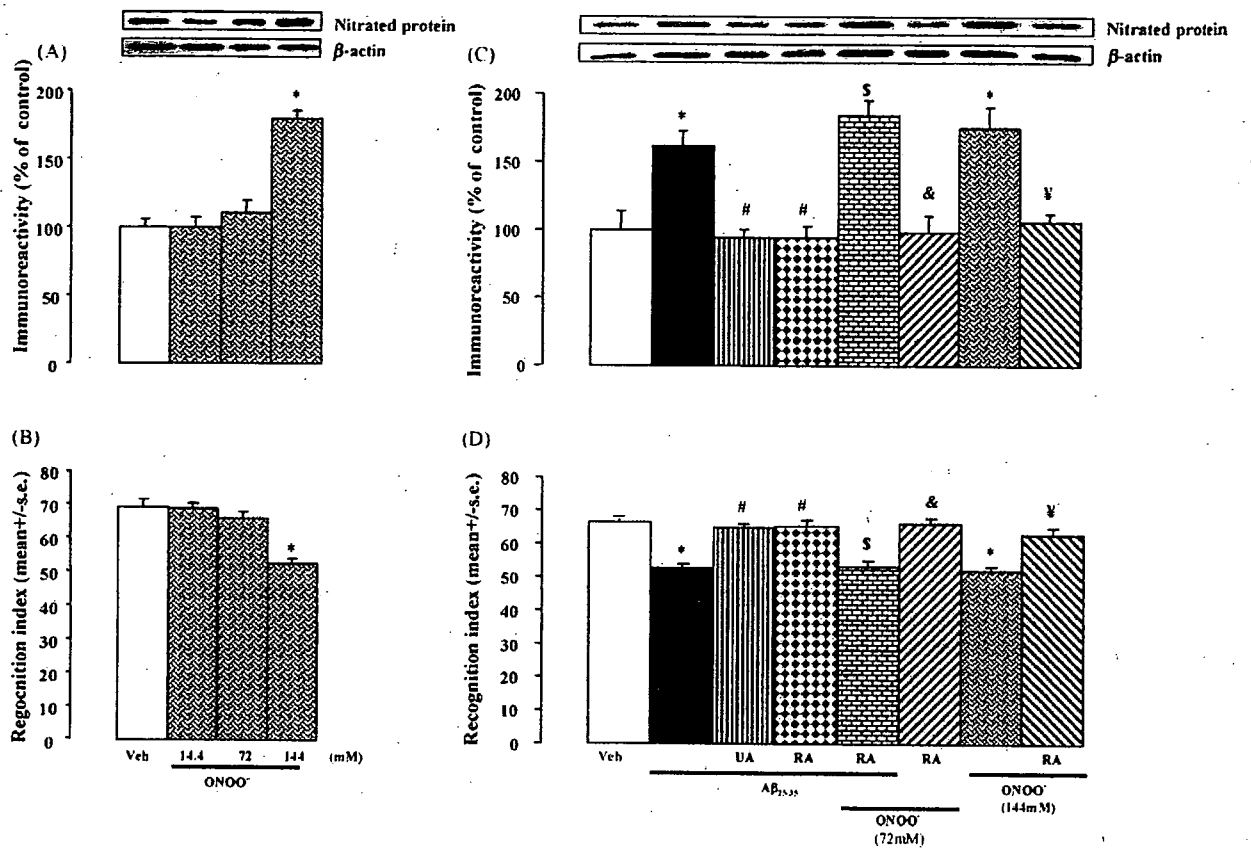

Fig. 4. The effects of rosmarinic acid on the nitration of proteins and the impairment of memory induced by $A\beta_{25-35}$ and $ONOO^-$. (A and B) i.c.v.-Injection of $ONOO^-$ nitrated hippocampal proteins and induced impairment of memory. (C and D) i.c.v.-Injection of $A\beta_{25-35}$ significantly increased the nitration of hippocampal proteins. RA (0.25 mg/kg day) manifested prevention of $A\beta_{25-35}$-induced protein nitration is not different from that of UA (100 mg/kg day), a scavenger of $ONOO^-$. Co-injection of a safe dose (72 mM) of $ONOO^-$ with $A\beta_{25-35}$ blocked the protective effects of RA. RA (0.25 mg/kg day) prevented the protein nitration and memory impairment induced by $ONOO^-$ (144 mM). Data were presented as the mean ± S.E. ($n = 10$). $^*p < 0.05$ vs. veh; $^{\#}p < 0.05$ vs. $A\beta_{25-35}$; $^{\$}p < 0.05$ vs. $A\beta_{25-35}$ + RA; $^{\&}p < 0.05$ vs. $A\beta_{25-35}$ + RA + $ONOO^-$; $^{¥}p < 0.05$ vs. $ONOO^-$. Veh: vehicle, RA: rosmarinic acid, $A\beta_{25-35}$: amyloid beta (25–35), UA: uric acid, $ONOO^-$: peroxynitrite.

$A\beta_{25-35}$-injected mice did not discriminate the novel and familiar objects by showing a significantly decreased exploration to the new object in a comparison with vehicle group. All doses (except 0.05 mg/kg) of RA significantly enhanced the new object discrimination ability of $A\beta_{25-35}$-injected mice (Fig. 3D). However, no dose dependent response was observed. The effective lowest dose (0.25 mg/kg) of RA did not boost memory function in normal mice (Fig. 3B and C), restricting its memory protecting effects to its anti-oxidant property. Therefore, the optimum dose of the memory protective effects of RA for the rest of the study was selected to be 0.25 mg/kg.

3.2. The effect of RA on the nitration of proteins

$ONOO^-$-mediated nitrative damage, which could be indirectly indicated by the nitration of proteins, seems to contribute much of the neurotoxicity of Aβ [4–6,34,35]. In vitro studies show that RA is a robust scavenger of $ONOO^-$ and other free radicals [8,32]. Thus, the protective effects of RA in our model seem to be involved in the scavenging of $ONOO^-$ induced by $A\beta_{25-35}$. To examine the direct involvement of $ONOO^-$ in the impairment of memory in our model, we tried the i.c.v.-injection of $ONOO^-$ itself. $ONOO^-$, at the concentration of 144 mM, but not at 72 mM, nitrated hippocampal proteins and induced impairment of memory (Fig. 4A and B). The i.c.v.-injection of $A\beta_{25-35}$ significantly increased the nitration of hippocampal proteins. Daily treatment with RA and uric acid (UA), a scavenger of peroxynitrite, prevented $A\beta_{25-35}$-induced protein nitration and memory impairment (Fig. 4C and D). However, co-injection of a non-memory-impairing dose (72 mM) of $ONOO^-$ with $A\beta_{25-35}$ blocked the preventive effects of RA in terms of protein nitration and impairment of memory. The protein nitration and memory impairment induced by $ONOO^-$ (144 mM) was prevented by the daily treatment with RA (Fig. 4C and D).

4. Discussion

AD is an age-related neurodegenerative disorder with progressive cognitive dysfunction and characterized by presence of senile plaques in the brain. Aβ is the major component of senile plaques and is considered to have a causal role in the development and progress of AD. *Intracerebroventricular* administration of $A\beta_{1-40}$ in rats causes memory deficits [20,24,25]. Etiological studies have indicated that oxidative

stress, an early event in the pathology of AD [26], is responsible for the onset of the cognitive dysfunction as well as the progression of the disease [5,14,34]. Elevated levels of Aβ, a natural antioxidant in physiological concentrations [15], induce oxidative stress which could mediate the damage seen in AD [4]. High levels of Aβ is responsible for the increased appearance of reactive oxygen species such as superoxide (O_2^-) and NO in AD [4,19,48]. The rapid interaction between O_2^- and NO produces $ONOO^-$, a general source of oxidative damage induced by Aβ in the brain of patients with AD [4,31]. $ONOO^-$ exhibits strong rapid damage including peroxidation of lipids and nitration of tyrosine residues of proteins, and thus affects cell function in many different ways. The $ONOO^-$-mediated damage, a wide spread phenomenon in AD brain, leads the onset of the disease [6,14,35]. Although the half-life of NO is extremely short, $ONOO^-$ is formed at a rate more than three times faster than the scavenging of superoxide by superoxide dismutase, suggesting criticality of the over-produced NO. Aβ induces the overproduction of NO via iNOS, and inhibition or ablation of the latter prevents the impairment of memory induced by $A\beta_{1-40}$ [23,41,42]. In the brains of both sporadic and familial AD patients, the number of inducible nitric oxide synthase (iNOS) positive neurons is conspicuously higher than in that of control patients [43]. It is obvious that the inhibition of iNOS to reduce $ONOO^-$ could be an ideal alternative to prevent the neurotoxicity of Aβ in AD. However, the involvement of iNOS in other pathological and physiological aspects of life makes the idea less feasible [11,13]. Therefore, the scavenging of peroxynitrites directly by using natural safe ingredients from the medicinal herbs could be a rational alternative of preventive and therapeutic interventions in the neurotoxicity of Aβ.

In this study, we have therefore investigated the effect of RA, a scavenger of $ONOO^-$, on the memory impairment induced by $A\beta_{25-35}$. We also examined the possible mechanism to explain the therapeutic property of RA through its $ONOO^-$-scavenging effects to prevent the nitration of proteins induced by $A\beta_{25-35}$. $A\beta_{25-35}$, at the dose of 3 μg/3 μl, did not produce the impairment of memory (in NORT) until Day 5 after its injection. The impairment of memory induced by $A\beta_{25-35}$ showed a gradual aggravation till Day 12 when evaluated in cue and contextual fear-conditioning test (unpublished data). The nitration of proteins was found relatively stronger (might be due to the rate of gradual formation and time-dependent clearance) on Day 5 than that on other time points and positively associated with the level of impairment of memory. When the nitration was prevented till Day 5, no impairment of memory was observed in behavioral tests on later time points (unpublished observation). Therefore, we selected the indicated time courses in this study. To determine the dose of RA which is sufficient to prevent the memory impairment induced by $A\beta_{25-35}$ in mice, several doses of RA were administered i.p. At the doses of 0.25, 1, 2, and 4 mg/kg, RA significantly prevented the $A\beta_{25-35}$-induced impairment of the alteration behavior as an immediate working memory in the Y maze test and the impairment of the ability of novel object discrimination as a long-term memory in the NORT. However, no dose-dependent response was observed. The lack of a dose-dependent effect of RA could be explained as follow: first, there is the ceiling effect of RA in the present behavioral tasks. Because it is hard to get 100% of alteration behavior and recognition index, since the chance level is 50% in both behavioral tasks. Second, RA is rapidly decreased in the blood circulation after intravenous administration ($t_{1/2} = 9$ min) [28]. A previous pharmacokinetic study has defined a number of metabolites of RA such as caffeic acid, ferulic acid and hydroxyphenylpropionic acid [22]. Among these, caffeic acid has been reported to inhibit the production and the release of NO in activated astrocytes and macrophages in culture studies [36,49]; ferulic acid, a further metabolite of caffeic acid, has been reported to protect against oxidative stress and memory impairment induced by Aβ [29,46]. These reports about the metabolism and metabolites of RA may explain the lack of dose response as well as the efficacy of RA at a very low dose of 0.25 mg/kg. Thus, the optimum dose of the protective effects of RA was selected to be 0.25 mg/kg for the rest of the study. The memory impairments seen in AD are contributed by Aβ-driven $ONOO^-$-mediated damages [34,35]. The memory protective effect of RA could be due to the capturing of the extremely noxious $ONOO^-$ induced of $A\beta_{25-35}$. To examine this, the involvement of $ONOO^-$ in the impairment of memory was confirmed by i.c.v.-injection of itself or daily treatment with UA, a scavenger of $ONOO^-$, after the injection of $A\beta_{25-35}$. $ONOO^-$ induced nitration of proteins and impaired the memory. UA prevented $A\beta_{25-35}$-induced nitration of proteins in the hippocampus and impairment of memory, indicating that the proxynitrites are the major contributors to the toxicity of $A\beta_{25-35}$. UA treatment in vehicle-treated group did not affect the memory (data not shown). RA prevented the $ONOO^-$-induced nitration of proteins and impairment of memory. Daily treatment with RA significantly prevented the nitration of proteins as well as memory impairment induced by $A\beta_{25-35}$. However, RA protection of $A\beta_{25-35}$ toxicity was abolished after the co-injection of non-memory impairing dose of proxynitrites to increase the proxynitrite burden. It was implied that the memory protecting effects of RA are due to its activity of scavenging proxynitrites. Indeed, proxynitrites-induced nitration of proteins and impairment of memory were prevented by daily treatment with RA. As for the increase of nitration of proteins by the co-injection, it might be that the pro-oxidative property of $A\beta_{25-35}$ may increase in the presence of proxynitrites, or the co-injected proxynitrites make the cells more vulnerable to the toxicity of $A\beta_{25-35}$. The results together indicated that the RA protects memory through the scavenging of $ONOO^-$ which induced by $A\beta_{25-35}$.

Although investigations about the activity of RA on central nervous system (CNS) are few, two lines of studies have shown the antidepressive-like activity of RA in mice exposed to conditioned fear stress and the forced swimming test [38,39]. Other unknown properties of RA and its metabolites in CNS may also contribute to its protective effects on the memory impairment induced by Aβ. Nevertheless, our study provided clear evidence that RA protects against the impairment of memory in the neurotoxicity of Aβ by preventing $ONOO^-$-mediated damage.

In summary, the results of this study and all other reported properties of RA strongly suggest its usefulness in the treatment of memory impairment observed in AD.

Acknowledgements

This work was supported, in part, by the Japan-China Sasakawa Medical fellowship (For Tursun Alkam); by Uehara Memorial Foundation fellowship for Foreign Researchers in Japan (For Tursun Alkam); by a Grant-in-Aid for the 21st Century Center of Excellence Program "Integrated Molecular Medicine for Neuronal and Neoplastic Disorders" from the Ministry of Education, Culture, Sports, Science and Technology of Japan; by a Grant-in-Aid for Health Science Research on Regulatory Science of Pharmaceuticals and Medical Devices, and Comprehensive Research on Aging and Health from the Ministry of Health, Labor and Welfare of Japan; by Japan Canada Joint Health Research Program (Joint Project from Japan Society for the Promotion of Science); by a grant from the Brain research Center from 21st Century Frontier Research Program funded by the Ministry of Science and Technology, Republic of Korea; and by a Smoking Research Foundation Grant for Biomedical Research.

References

[1] Akhondzadeh S, Noroozian M, Mohammadi M, Ohadinia S, Jamshidi AH, Khani M. *Melissa officinalis* extract in the treatment of patients with mild to moderate Alzheimer's disease: a double blind, randomised, placebo controlled trial. J Neurol Neurosurg Psychiatry 2003;74:863–6.

[2] Akhondzadeh S, Noroozian M, Mohammadi M, Ohadinia S, Jamshidi AH, Khani M. *Salvia officinalis* extract in the treatment of patients with mild to moderate Alzheimer's disease: a double blind, randomized and placebo-controlled trial. J Clin Pharmacol Ther 2003;28:53–9.

[3] Bandoniene D, Murkovic M, Venskutonis PR. Determination of rosmarinic acid in sage and borage leaves by high-performance liquid chromatography with different detection methods. J Chromatogr Sci 2005;43:372–6.

[4] Butterfield DA. Aβ-associated free radical oxidative stress and neurotoxicity: implications for Alzheimer's disease. Chem Res Toxicol 1997;10:495–506.

[5] Butterfield DA, Drake J, Pocernich C, Castegna A. Evidence of oxidative damage in Alzheimer's disease brain: central role for Aβ. Trends Mol Med 2001;7:548–54.

[6] Castegna A, Thongboonkerd V, Klein JB, Lynn B, Markesbery WR, Butterfield DA. Proteomic identification of nitrated proteins in Alzheimer's disease brain. J Neurochem 2003;85:1394–401.

[7] Cheng G, Whitehead SN, Hachinski V, Cechetto DF. Effects of pyrrolidine dithiocarbamate on $A\beta_{25-35}$-induced inflammatory responses and memory deficits in the rat. Neurobiol Dis 2006;23:140–51.

[8] Choi HR, Choi JS, Han YN, Bae SJ, Chung HY. Peroxynitrite scavenging activity of herb extracts. Phytother Res 2002;16:364–7.

[9] Dodart JC, Bales KR, Gannon KS, Greene SJ, DeMattos RB, Mathis C, et al. Immunization reverses memory deficits without reducing brain Abeta burden in Alzheimer's disease model. Nat Neurosci 2002;5:452–7.

[10] Ennaceur A, Delacour J. A new one-trial test for neurobiological studies of memory in rats. 1. Behavioral data. Behav Brain Res 1998;31:47–59.

[11] Gonzalez-Cadavid NF, Rajfer J. The pleiotropic effects of inducible nitric oxide synthase (iNOS) on the physiology and pathology of penile erection. Curr Pharm Des 2005;11:4041–6.

[12] Iuvone T, De Filippis D, Esposito G, D'Amico A, Izzo AA. The spice sage and its active ingredient rosmarinic acid protect PC12 cells from Aβ-induced neurotoxicity. J Pharmacol Exp Ther 2006;317:1143–9.

[13] Kalinchuk AV, Stenberg D, Rosenberg PA, Porkka-Heiskanen T. Inducible and neuronal nitric oxide synthases (NOS) have complementary roles in recovery sleep induction. Eur J Neurosci 2006;24:1443–56.

[14] Keller JN, Schmitt FA, Scheff SW, Ding Q, Chen Q, Butterfield DA, et al. Evidence of increased oxidative damage in subjects with mild cognitive impairment. Neurology 2005;64:1152–6.

[15] Kontush A. Aβ: an antioxidant that becomes a pro-oxidant and critically contributes to Alzheimer's disease. Free Radic Biol Med 2001;31:1120–31.

[16] Lamaison JL, Petitjean-Freytet C, Carnat A. Medicinal Lamiaceae with antioxidant properties, a potential source of rosmarinic acid. Pharm Acta Helv 1991;66:185–8.

[17] Maurice T, Lockart BP, Private A. Amnesia induced by centrally administered Aβ peptides involves cholinergic dysfunction. Brain Res 1996;706:181–93.

[18] Moreno S, Scheyer T, Romano CS, Vojnov AA. Antioxidant and antimicrobial activities of rosemary extracts linked to their polyphenol composition. Free Radic Res 2006;40:223–31.

[19] McLellan ME, Kajdasz ST, Hyman BT, Bacskai BJ. In vivo imaging of reactive oxygen species specifically associated with thioflavine S-positive amyloid plaques by multiphoton microscopy. J Neurosci 2003;23:2212–7.

[20] Nabeshima T, Nitta A. Memory impairment and neuronal dysfunction induced by Aβ protein in rats. Tohoku J Exp Med 1994;174:241–9.

[21] Gao LP, Wei HL, Zhao HS, Xiao SY, Zheng RL. Antiapoptotic and antioxidant effects of rosmarinic acid in astrocytes. Pharmazie 2005;60:62–5.

[22] Nakazawa T, Ohsawa K. Metabolism of rosmarinic acid in rats. J Nat Prod 1998;61:993–6.

[23] Nathan C, Calingasan N, Nezezon J, Ding A, Lucia MS, La Perle K, et al. Protection from Alzheimer's-like disease in the mouse by genetic ablation of inducible nitric oxide synthase. J Exp Med 2005;202:1163–9.

[24] Nitta A, Itoh A, Hasegawa T, Nabeshima T. Aβ protein-induced Alzheimer's disease animal model. Neurosci Lett 1994;170:63–6.

[25] Nitta A, Fukuta T, Hasegawa T, Nabeshima T. Continuous infusion of Aβ protein into the rat cerebral ventricle induces learning impairment and neuronal and morphological degeneration. Jpn J Pharmacol 1997;73:51–7.

[26] Nunomura A, Perry G, Aliev G, Hirai K, Takeda A, Balraj EK, et al. Oxidative damage is the earliest event in Alzheimer disease. J Neuropathol Exp Neurol 2001;60:759–67.

[27] Ono K, Hasegawa K, Naiki H, Yamada M. Curcumin has potent anti-amyloidogenic effects for Alzheimer's Aβ fibrils in vitro. J Neurosci Res 2004;75:742–50.

[28] Parnham MJ, Kesselring K. Rosmarinic acid. Drugs Future 1985;10:756–7.

[29] Perluigi M, Joshi G, Sultana R, Calabrese V, De Marco C, Coccia R, et al. In vivo protective effects of ferulic acid ethyl ester against $A\beta_{1-42}$-induced oxidative stress. J Neurosci Res 2006 [Epub ahead of print].

[30] Pike CJ, Walencewicz-Wasserman AJ, Kosmoski J, Cribbs DH, Glabe CG, Cotman CW. Structure–activity analyses of Aβ peptides: contributions of the β_{25-35} region to aggregation and neurotoxicity. J Neurochem 1995;64:253–65.

[31] Poon HF, Joshi G, Sultana R, Farr SA, Banks WA, Morley JE, et al. Antisense directed at the Abeta region of APP decreases brain oxidative markers in aged senescence accelerated mice. Brain Res 2004;1018:86–96.

[32] Qiao S, Li W, Tsubouchi R, Haneda M, Murakami K, Takeuchi F, et al. Rosmarinic acid inhibits the formation of reactive oxygen and nitrogen species in RAW264.7 macrophages. Free Radic Res 2005;39:995–1003.

[33] Sanbongi C, Takano H, Osakabe N, Sasa N, Natsume M, Yanagisawa R, et al. Rosmarinic acid inhibits lung injury induced by diesel exhaust particles. Free Radic Biol Med 2003;34:1060–9.

[34] Smith MA, Perry G, Richey PL, Sayre LM, Anderson VE, Beal MF, et al. Oxidative damage in Alzheimer's. Nature 1996;382:120–1.

[35] Smith MA, Richey Harris PL, Sayre LM, Beckman JS, Perry G. Widespread peroxynitrite-mediated damage in Alzheimer's disease. J Neurosci 1997;17:2653–7.

[36] Soliman KF, Mazzio EA. In vitro attenuation of nitric oxide production in C6 astrocyte cell culture by various dietary compounds. Proc Soc Exp Biol Med 1998;218:390–7.

[37] Takano H, Osakabe N, Sanbongi C, Yanagisawa R, Inoue K, Yasuda A, et al. Extract of *Perilla frutescens* enriched for rosmarinic acid, a polyphenolic phytochemical, inhibits seasonal allergic rhinoconjunctivitis in humans. Exp Biol Med 2004;229:247–54.

[38] Takeda H, Tsuji M, Inazu M, Egashira T, Matsumiya T. Rosmarinic acid and caffeic acid produce antidepressive-like effect in the forced swimming test in mice. Eur J Pharmacol 2002;449:261–7.

[39] Takeda H, Tsuji M, Miyamoto J, Matsumiya T. Rosmarinic acid and caffeic acid reduce the defensive freezing behavior of mice exposed to conditioned fear stress. Psychopharmacology 2002;164:233–5.
[40] Tohda C, Matsumoto N, Zou K, Meselhy MR, Komatsu K. $A\beta_{25-35}$ induced memory impairment, axonal atrophy, and synaptic loss are ameliorated by M1, a metabolite of protopanaxadiol-type saponins. Neuropsychopharmacology 2004;29:860–8.
[41] Tran MH, Yamada K, Nakajima A, Mizuno M, He J, Kamei H, et al. Tyrosine nitration of a synaptic protein synaptophysin contributes to Aβ-peptide-induced cholinergic dysfunction. Mol Psychiatry 2003;8: 407–12.
[42] Tran MH, Yamada K, Olariu A, Mizuno M, Ren XH, Nabeshima T. Aβ-peptide induces nitric oxide production in rat hippocampus: association with cholinergic dysfunction and amelioration by inducible nitric oxide synthase inhibitors. FASEB J 2001;15:1407–9.
[43] Vodovotz Y, Lucia MS, Flanders KC, Chesler L, Xie QW, Smith TW, et al. Inducible nitric oxide synthase in tangle-bearing neurons of patients with Alzheimer's disease. J Exp Med 1996;184:1425–33.
[44] Wang H, Xu H, Dyck LE, Li XM. Olanzapine and quetiapine protect PC12 cells from $A\beta_{25-35}$-induced oxidative stress and the ensuing apoptosis. J Neurosci Res 2005;81:572–80.
[45] Yamada K, Noda Y, Hasegawa T, Komori Y, Nikai T, Sugihara H, et al. The role of nitric oxide in dizocilpine-induced impairment of spontaneous alternation behaviorin mice. J Pharmacol Exp Ther 1996;276:460–6.
[46] Yan JJ, Cho JY, Kim HS, Kim KL, Jung JS, Huh SO, et al. Protection against Aβ peptide toxicity in vivo with long-term administration of ferulic acid. Br J Pharmacol 2001;133:89–96.
[47] Yankner BA, Duffy LK, Kirschner DA. Neurotrophic and neurotoxic effects of Aβ protein: reversal by tachykinin neuropeptides. Science 1990;250:279–82.
[48] Yatin SM, Varadarajan S, Link CD, Butterfield DA. In vitro and in vivo oxidative stress associated with Alzheimer's $A\beta_{1-42}$. Neurobiol Aging 1999;20:325–30.
[49] Yokozawa T, Chen CP. Role of *Salviae Miltiorrhizae Radix* extract and its compounds in enhancing nitric oxide expression. Phytomedicine 2000;7:55–61.

Available online at www.sciencedirect.com
ScienceDirect
Behavioural Brain Research 180 (2007) 152–160
BEHAVIOURAL BRAIN RESEARCH
www.elsevier.com/locate/bbr

Research report

Hypofunctional glutamatergic neurotransmission in the prefrontal cortex is involved in the emotional deficit induced by repeated treatment with phencyclidine in mice: Implications for abnormalities of glutamate release and NMDA–CaMKII signaling

Rina Murai [a], Yukihiro Noda [a,b], Kanae Matsui [a,c], Hiroyuki Kamei [c], Akihiro Mouri [a], Kazuhisa Matsuba [c], Astumi Nitta [a], Hiroshi Furukawa [d], Toshitaka Nabeshima [a,*]

[a] *Department of Neuropsychopharmacology and Hospital Pharmacy, Nagoya University Graduate School of Medicine, 65 Tsuruma-cho, Showa-ku, Nagoya 466-8560, Japan*
[b] *Division of Clinical Science and Neuropsychopharmacology in Clinical Pharmacy Practice, Management and Research, Faculty of Pharmacy, Meijo University, Nagoya 468-8503, Japan*
[c] *Department of Health-Care Pharmacy, Laboratory of Clinical Pharmacy Practice and Health Care Management, Faculty of Pharmacy, Meijo University, Nagoya 468-8503, Japan*
[d] *Department of Medical Chemistry, Faculty of Pharmacy, Meijo University, Nagoya 468-8503, Japan*

Received 30 January 2007; received in revised form 26 February 2007; accepted 2 March 2007
Available online 12 March 2007

Abstract

In the present study, we investigated the involvement of prefrontal glutamatergic neurotransmission in the enhancement of immobility (emotional deficit) in a forced swimming test in mice treated with phencyclidine (PCP: 10 mg/kg/day for 14 days) repeatedly, which is regarded as an animal model for negative symptoms. A decrease in spontaneous extracellular glutamate release and increase in levels of the glutamate transporter GLAST, were observed in the prefrontal cortex (PFC) of PCP-treated mice, compared to saline-treated mice. NMDA receptor subunit 1 (NR1) and Ca^{2+}/calmoduline kinase II (CaMKII) were markedly activated in the PFC of saline-treated mice, but not PCP-treated mice, immediately after the forced swimming test. The facilitation of the function of NMDA receptors by D-cycloserine (30 mg/kg i.p.), an NMDA receptor glycine-site partial agonist, reversed the enhancement of immobility in the forced swimming test and impairment of CaMKII activation in the PCP-treated mice. Microinjection of DL-threo-β-benzyloxyaspartate (10 nmol/site/bilaterally), a potent blocker of glutamate transporters, into the PFC of PCP-treated mice also had an attenuating effect. In addition, activation of glial cells and a decrease of neuronal cell size were observed in the PFC of PCP-treated mice. These results suggest that repeated PCP treatment disrupts pre- and post-synaptic glutamatergic neurotransmission and induces morphological changes in the PFC and that such changes cause the emotional deficits exhibited in PCP-treated mice.

Keywords: Phencyclidine; Emotional deficit; *N*-Methyl-D-aspartate; Prefrontal cortex; Glutamate; CaMKII

1. Introduction

Alternations of glutamatergic systems involving NMDA receptors are relevant to the pathophysiology of schizophrenia as demonstrated by pharmacological evidence that NMDA receptor antagonists reproduce some symptoms of the disease in normal individuals: phencyclidine (PCP), a non-competitive *N*-methyl-D-aspartate (NMDA) receptor antagonist, has been shown to induce schizophrenia-like psychosis representing positive symptoms, negative symptoms, and cognitive deficits in humans [17], which persist several weeks after withdrawal from chronic PCP use [1,25,42]. D-Cycloserine, a partial NMDA receptor glycine-site agonist, provides a modest improvement of even the cognitive deficits and negative symptoms in schizophrenia [8,17]. Chronic PCP psychosis might be more consistent with schizophrenia than acute PCP psychosis [17,21].

We have previously reported that chronic treatment with PCP (10 mg/kg/day s.c. for 14 days) induces several schizophrenia-

* Corresponding author. Tel.: +81 52 744 2674; fax: +81 52 744 2682.
E-mail address: tnabeshi@med.nagoya-u.ac.jp (T. Nabeshima).

0166-4328/$ – see front matter © 2007 Elsevier B.V. All rights reserved.
doi:10.1016/j.bbr.2007.03.003

like behavioral abnormalities such as an enhancement of immobility in a forced swimming test [36–38], social deficits [41] in a social interaction test, associative learning impairment in cued and contextual fear conditioning [11] in mice. Therefore, PCP-treated mice might be a useful model of schizophrenia [11,19,22,28,36–38,41].

It is hypothesized that insufficient glutamate neurotransmission in the PFC is associated with the pathology of schizophrenia [3,4,13]. Abnormal glutamatergic systems in the PFC have been found in PCP-treated mice, i.e. altered expression of the NMDA receptor subunit or an associated protein and decreased metabolic activity [7]. NMDA receptors are composed of at least one NR1 subunit and one or more modulatory subunits and regulate various forms of neuronal plasticity. NR1 knockdown and NR2A knockout mice have been reported to show schizophrenia-like behavioral abnormalities such as hyperactivity and social withdrawal [15,31,32]. However, little attempt has been made to investigate the involvement of prefrontal glutamatergic neurotransmission via NMDA receptors in negative symptom-like emotional deficits in PCP-treated mice.

In this article, we describe the results of experiments designed to test the hypothesis that the negative symptom-like emotional deficit in a forced swimming test is mediated via impaired pre- and post-synaptic glutamatergic neurotransmission in the PFC of mice treated with PCP repeatedly. We attempted to investigate the changes in (1) NMDA-Ca^{2+}/calmodulin-dependent protein (CaMKII) signaling after the forced swimming test, since the NMDA receptor and CaMKII form a tight complex at synapses which may facilitate the activation of second messenger pathways [10,26], (2) extracellular glutamate levels, (3) the expression levels of glutamate transporters, and (4) morphology of neurons and glia in the PFC. We also examined the effect of (5) facilitation of the function of NMDA receptors by D-cycloserine, an NMDA receptor glycine-site agonist, and DL-threo-β-benzyloxyaspartate (DL-TBOA), a non-substrate glutamate transport inhibitor, on behavioral and biochemical abnormalities in PCP-treated mice.

2. Materials and methods

2.1. Animals

Male mice of the ddY strain (Japan SLC Inc., Shizuoka, Japan), weighing 30–33 g at the beginning of the experiments, were used. The animals were housed in plastic cages and kept in a regulated environment (23 ± 1 °C, 50 ± 5% humidity), with a 12/12 h light–dark cycle (lights on at 8:00 a.m.). Food (CE2; Clea Japan Inc., Japan) and tap water were available ad libitum. All animal care and use was in accordance with the National Institutes of Health Guide for the Care and Use of Laboratory Animals and was approved by the Institutional Animal Care and Use Committee of Nagoya University School of Medicine.

2.2. Drugs

Phencyclidine hydrochloride (PCP) was synthesized by the authors according to the method of Maddox et al. [27] and was checked for purity. D-Cycloserine (Sigma, MO) and PCP were dissolved in a 0.9% NaCl solution. DL-TBOA (Tocris, MO) was prepared as a stock solution of 100 mM in 50% dimethyl sulfoxide (DMSO) and 100 mM NaOH, and dissolved in phosphate-buffered saline (PBS) before the experiments. KN93 and KN92 were purchased from Sigma–Aldrich and dissolved in a 0.01% DMSO (dimethyl sulfoxide)-containing saline solution.

2.3. Drug treatment

The mice were administered saline or PCP (10 mg/kg/day s.c.) once a day for 14 consecutive days. They were injected with D-cycloserine (s.c.) or DL-TBOA 30 min and KN93 or KN92 10 min before the measurement of immobility in the forced swimming test. DL-TBOA (1 or 10 nmol/site/bilaterally), KN93 (10 nmol/site/bilaterally), and KN92 (10 nmol/site/bilaterally) were microinjected into the PFC [anteroposterior (AP): 1.7, mediolateral (ML): ±0.5 from bregma, dorsoventral (DV): 2 mm from the skull] according to the mouse brain atlas of Franklin and Paxinos [14]. Dual 27-gauge microinjectors attached to tubing were inserted through the guides, from which they protruded 2.5 mm. The other end of the tubing was connected to a 25 μl Hamilton syringe. The volumes were injected over a period of about 30 s, and the injector was left in place for 1 min to allow diffusion. All compounds except for DL-TBOA, KN93 and KN92 were administered in a volume of 0.1 ml/10 g body weight.

2.4. Forced swimming test

The forced swimming test was done according to previous reports [36–38] with a minor modification. The test was performed the day after the final treatment with PCP. Namely, each mouse was placed in a transparent glass cylinder (20 cm high, 15 cm in diameter), which contained water at 22–23 °C to a depth of 15 cm, and was forced to swim for 180 s. The duration of swimming was measured, by using a SCANET MV-10 AQ apparatus (Melquest Co. Ltd., Japan). The immobility time was calculated as follows: 180 (s) − swimming time (s) = immobility time (s).

2.5. Microdialysis analysis

On day 14 after the start of PCP treatment, the mice were anesthetized with pentobarbital Na (50 mg/kg i.p.) and fixed in a stereotaxic apparatus (David Kopf Instruments, CA). A guide cannula (AG-6 EICOM, Japan) was implanted into the PFC [15° angle away from AP: +1.7, ML: −1.0 from bregma, DV: −1.5 mm from the skull] according to the atlas. On day 15 (24 h after the implantation of the guide cannula: 1 day after PCP withdrawal), a dialysis probe (A-I-6-01; membrane length 1 mm, EICOM, Japan) was implanted into the PFC and Ringer solution (147 mM, NaCl, 4 mM KCl, and 2.3 mM $CaCl_2$) was perfused at a flow rate of 1.0 μl/min. The dialysate was colleted every 10 min and the amount of glutamate in the dialysate was determined using an HPLC system (HTEC-500, EICOM, Japan) with electrochemical detection (ECD). Three samples were taken to establish baseline levels of extracellular glutamate. For depolarization stimulation, 100 mM KCl-containing Ringer solution was delivered through the dialysis probe for 30 min in order to induce the K^+-evoked release of glutamate. Then dialysate was collected for 70 min with Ringer solution. For the rescue study with DL-TBOA, a dialysis probe equipped with a microinjection tube (MIA-6-1; 1 mm membrane length, EICOM) was used. After the collection of baseline fractions, 10 nmol of DL-TBOA dissolved in 1 μl of PBS was injected bilaterally during a 10-min period through the microinjection tube into the PFC.

2.6. Western blotting

Western blotting was performed as described [11] with a minor modification. Immediately after the forced swimming test, the mice were sacrificed by decapitation. The PFC containing cingulate and prelimbic area (Bregma +2.96 to Bregma +1.34) defined as in Franklin and Paxinos was rapidly dissected out, frozen, and stored at −80 °C until used. The brain samples were homogenized in ice-cold buffer [50 mM Tris–HCl, pH 7.5; 150 mM NaCl; 10 mM NaF; 10 mM EDTA, 1% NP-40; 1 mM sodium orthovanadate; 10 mM sodium pyrophosphate; 0.5 mM DTT; 0.2 mM PMSF; 4 μg/ml pepstatin, 4 μg/ml aprotinin, and 4 μg/ml leupeptin for measuring phospho-NR1, NR1, phospho-Ca^{2+}/calmoduline kinase II (CaMK II), CaMKII, GLT-1, GLAST and actin]. The lysate was centrifuged at 8000 × g for 10 min at 4 °C. The protein concentration of the supernatant was determined by a Bradford assay (Bio-rad, CA). Sample buffer [0.25% bromophenol blue/0.25% xylene cyanol 30% glycerol/20% 2× Tris–borate EDTA

(90 mM Tris/64.6 mM boric acid/2.5 mM EDTA, pH 8.4)] was added to the supernatant and the mixture was boiled at 95 °C for 5 min. Equivalent amounts of protein (20 μg) were electrophorated on SDS-polyacrylamide gels, transferred to PVDF membranes (Millipore, MA), and blocked with a Detector Block Kit (KPL, MD). The membranes were incubated with a rabbit anti-phospho-NR1 (S897), a rabbit anti-phospho CaMKII (1:1000; Upstate Biotechnology), a guinea-pig anti-GLAST (1:1000; Chemicon, CA), a guinea-pig anti-GLT-1 (1:1000; Oncogene, MA) or an anti-actin (C-11) (1:1000; Santa Cruz Biotechnology, CA) antibody at 4 °C overnight. For the analysis of phospho-CaMKII, CaMKII, GLAST and GLT-1 levels, each protein was boiled in a sample buffer and a 10% polyacrylamide gel and subsequently transferred to a polyvinylidine difluoride membrane (Millipore) and blocked with a Detector Block kit (KPL). The membranes were then washed with washing buffer (50 mM Tris–HCl, pH 7.4, and 150 mM NaCl and 0.05% Tween 20). After incubation with a 1:1000 dilution of horseradish peroxidase (HRP)-conjugated IgG for 2 h, the membranes were washed with washing buffer. The immune complex was detected using an enhanced chemiluminscence (ECL) kit (Amersham Pharmacia Biotech Inc., NJ) and exposed to X-ray film. Images on the film were captured using a CCD camera (ATTO, Japan). The intensity of each band was analyzed quantitatively using the ATTO Densitograph Software Library Lane Analyzer (ATTO). To measure total (phospho- and non-phospho-) NR1 or CaMKII, membranes were stripped with stripping buffer (100 mM 2-melcaptoethanol; 2% SDS; and 62.5 mM Tris–HCl, pH 6.7) at 50 °C for 30 min, and incubated with a mouse anti-NR1 CT (1:1000; Upstate Biotechnology, NY) or a rabbit anti-CaMKII (1:1000; Sigma) antibody at 4 °C overnight. To evaluate NR-1 or CaMKII activation, phospho-NR-1 or CaMKII levels were normalized to total NR-1 or CaMKII levels in the same membranes, and then each phospho-/total-level was normalized to the basal phospho-/total-level in saline-treated mice. To evaluate the expression of GLAST and GLT-1, the GLAST and GLT-1 levels were normalized to the actin levels in the same membranes, and then GLAST/actin and GLT-1/actin levels were normalized to the GLAST/actin and GLT-1/actin levels in saline-treated mice.

2.7. Preparation of brain slice and staining

Histological procedures were performed as previously described with a minor modification [11,34]. Before and immediately after the forced swimming test, mice were anesthetized with chloral hydrate (200 mg/kg i.p.) and perfused transcardially with ice-cold phosphate-buffered saline (PBS), followed by 4% paraformaldehyde in PBS. The brains were removed, postfixed in the same fixative for 2 h, and then soaked in 20% (w/v) sucrose in PBS. Coronal sections 20 μm thick were cut with a cryostat (CM 1850; Leica, Germany). For immunohistochemistry, the primary antibodies that were applied in the brain slices included anti-GLAST (1:300), a guinea-pig anti-GLT-1 (1:300; Chemicon), a rabbit anti-s100 (1:300; Dako, CA) and mouse anti-GFAP (1:300; Chemicon) antibody. Fluorescently conjugated secondary antibodies (Alexa 488, 546; Molecular Probes, OR) were used for detecting chromagen. Twenty sections at 80 μm intervals from Bregma +2.96 to Bregma +1.34 were used from each brain, and prelimbic area was defined as in Franklin and Paxinos. For counting the number and calculate the size of neuron, Cresyl Violet staining was performed and only neurons with a visible nucleus and in which the entire outline of the cell was apparent were counted in standardized area in the prelimbic area using computer-based image analysis system (Image J, Bethesda, MD). Using these measurements, the surface area (μm^2) of s100-stained process and size of neuron, was calculated in standardized area in the layer II/III of the prelimbic area. Images were acquired with a confocal microscope (μ Radiance, Bio-Rad) provided by Division for Medical Research Engineering of Nagoya University or a light microscope (Axioskop2 plus; Carl Zeiss, Germany).

2.8. Statistical analysis

Statistical analysis was performed with a one-way analysis of variance (ANOVA) using Bonferroni's test. The unpaired *t*-test (Student's *t*-test) was used to compare two sets of data. A value of $p < 0.05$ was considered statistically significant. Data were expressed as the mean ± S.E.M.

3. Results

3.1. Ability to release glutamate in the prefrontal cortex

We examined the extracellular glutamate levels in the PFC of the PCP-treated mice by using an *in vivo* microdialysis technique. After the basal extracellular levels of glutamate reached a steady state, basal release of glutamate was monitored during 30 min of dialysis. PCP-treated mice showed a dramatically decreased basal level of glutamate in the PFC [PCP-treated mice: 0.905 ± 0.158 pmol/sample ($n = 6$), saline-treated mice: 4.26 ± 54.9 pmol/sample ($n = 5$)] (**Fig. 1**). We investigated the ability to release glutamate of high potassium (high K^+) (100 mM) in the PFC of the PCP-treated mice. The amount of glutamate released in the PFC of the PCP-treated mice was significantly less than that released the saline-treated mice ($p < 0.01$) [PCP-treated mice: 3.02 ± 0.28 pmol/sample ($n = 6$), saline-treated mice: 8.42 ± 0.90 pmol/sample ($n = 5$)] (**Fig. 1**), though the high K^+-induced extracellular glutamate release (% of baseline) in PCP-treated mice was about three-fold higher than that in saline-treated mice.

3.2. The changes of glutamate transporters, glial cells and neuronal morphology in the prefrontal cortex

Glial glutamate transporters, i.e. GLAST and GLT-1, play an important role in regulating glutamate transmission by rapidly

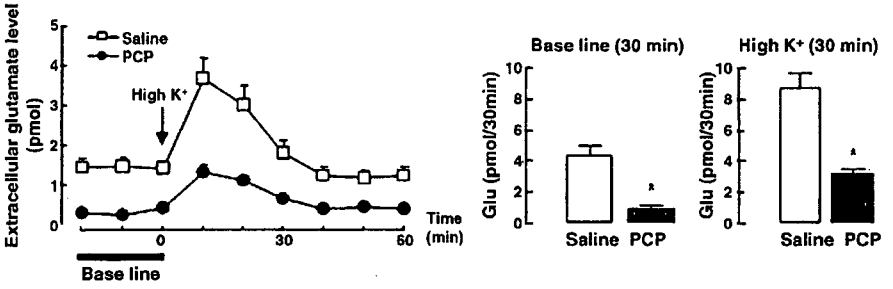

Fig. 1. Basal extracellular levels of glutamate and K^+-evoked glutamate release in the prefrontal cortex of mice treated with phencyclidine repeatedly. The mice were administered saline or phencyclidine (PCP: 10 mg/kg/day s.c.) for 14 days ($n = 5$ for saline-treated mice, $n = 6$ for PCP-treated mice). Basal extracellular levels of glutamate and K^+-evoked (100 mM) glutamate release in the prefrontal cortex (PFC) of saline- or PCP-treated mice were determined by a microdialysis method. Fractions were collected for 30 min. Basal extracellular glutamate levels were: PCP-treated mice, 0.91 ± 0.16 pmol/sample ($n = 6$); saline-treated mice, 4.26 ± 54.9 pmol/sample ($n = 5$). Values correspond to the mean ± S.E.M. $^*p < 0.05$ vs. saline-treated mice (Student's *t*-test). Glu: glutamate.

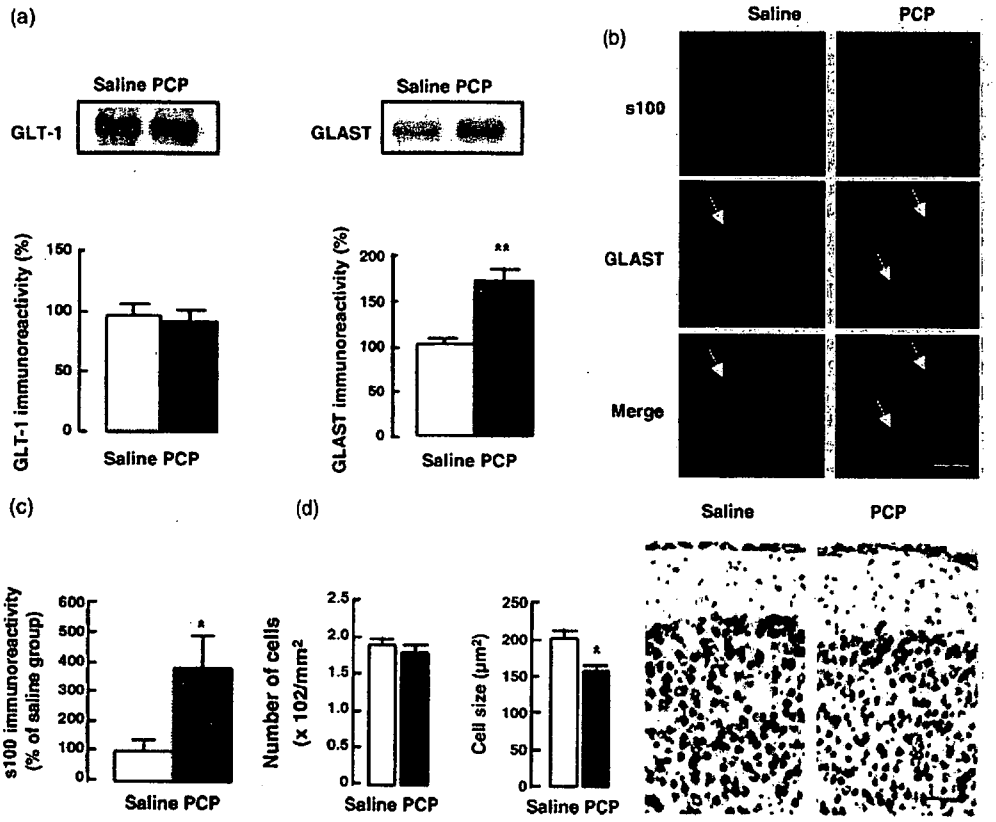

Fig. 2. The changes in expression of glutamate transporters and gross morphology in the prefrontal cortex of mice treated with phencyclidine repeatedly. The mice were administered saline or phencyclidine (PCP: 10 mg/kg/day s.c.) for 14 days. (a) Representative western blots and immunoreactivity to GLAST and GLT-1 in the prefrontal cortex (PFC) (GLAST: $n = 8$ in each group, GLT-1; $n = 6$ in each group). (b) Representative image of s100 (green) and GLAST (red) immunostained sections from the PFC of saline- and PCP-treated mice. Arrows indicates GLAST fluorescent puncta on the process of glia. Scale bar: 50 μm. (c) Stereological analysis of s100 immunoreactivity in the PFC of saline- and PCP-treated mice ($n = 4$ in each group). (d) Cresyl violet-stained coronal sections of the PFC and stereological analysis of cell number and cell size in the PFC of saline- and PCP-treated mice ($n = 5$ in each group). Scale bar: 200 μm. Values correspond to the mean ± S.E.M. $^{*}p < 0.05$, $^{**}p < 0.01$ vs. saline-treated mice (Student's t-test). Glu: glutamate.

clearing glutamate from extracellular fluid [9]. In order to examine whether the decrease in the extracellular concentration of glutamate is due to changes of glutamate transporters, we investigated the protein levels of glial glutamate transporters in the PFC of PCP-treated mice by immunoblotting. Although there was no difference in the GLT-1 protein level between PCP-treated mice and saline-treated mice, the expression level of GLAST protein was higher in the PCP-treated mice ($p < 0.01$; Fig. 2a).

Since immunoblot analysis showed an increase of GLAST levels, the localization of GLAST in the PFC of PCP-treated mice was analyzed by immunohistochemical methods. GLAST was localized to the processes of cells positive for s100, a glial marker, and merged with s100, both in saline-treated and in PCP-treated mice (Fig. 2b). The morphology of s100-positive cells was altered to the activated form with thick processes in the PCP-treated mice (Fig. 2b and c).

Glia is activated in response to several pathological conditions, such as physical or biochemical damage to the nervous tissue. To investigate whether repeated PCP treatment induces neuronal damage in the PFC, we examined morphological changes in neurons by Cresyl Violet staining. No difference in the number of neurons in the layer II/III of the PFC was observed regardless of PCP treatment (Fig. 2d). However, a decrease in neuronal cell size was revealed in the layer II/III of the PFC of PCP-treated mice compared to saline-treated mice (Fig. 2d).

3.3. Intracellular signaling via NMDA receptors in the prefrontal cortex

We investigated the change in the activation of CaMKII signaling via NMDA receptors in the PFC after the forced swimming test. The phosphorylation levels of NR1, one of the subunit of NMDA receptors, and of CaMKII, in the PFC of the saline-treated mice were significantly increased immediately after the test, compared to those in the non-tested, saline-treated mice ($p < 0.01$; Fig. 3a and b). However, the phosphorylation levels of NR1 (p-NR1) and CaMKII (p-CaMKII) did not increase after the test in the PCP-treated mice (Fig. 3a and b). There was no significant difference in p-NR1 and p-CaMKII between non-tested, saline- and PCP-groups. No difference in total NR1 and CaMKII expression levels was observed between the saline- and PCP-treated mice [NR1: $F(3, 15) = 1.54$, $p = 0.26$; CaMKII: $F(3, 31) = 0.68$, $p = 0.56$] (data not shown).